BIBLIOGRAPHIC DATA SHEET	1. Report No. EPA-R2-72-023	2.	3. Recipient's Accession No. PB-211 853
4. Title and Subtitle: Cyclic Operation of Plate Columns for Gas-Liquid Contacting			5. Report Date: May 1, 1972 6.
7. Author(s): James D. Dearth, Lawrence B. Evans, Edwin R. Gilliland			8. Performing Organization Rept. No.
9. Performing Organization Name and Address: Massachusetts Institute of Technology Department of Chemical Engineering Cambridge, Massachusetts			10. Project/Task/Work Unit No. Order No. 2 11. Contract/Grant No. 68-02-0018
12. Sponsoring Organization Name and Address: ENVIRONMENTAL PROTECTION AGENCY Control Systems Division Research Triangle Park, North Carolina 27711			13. Type of Report & Period Covered 14.

15. Supplementary Notes

16. Abstracts: Previous experimental and theoretical work has indicated that the efficiency and capacity of gas-liquid contacting equipment may be improved by controlled-cycling of gas and liquid flows. However, difficulties encountered in the design of large-scale systems, where hydraulic instabilities and axial liquid mixing effects have been found to be severe, has prevented wide-scale application of such systems to industrial separations. This report describes a proposed program for obtaining needed information on tray hydraulics and liquid mixing, and summarizes some initial data and tentative conclusions for both steady-state and cyclic flows of an air-water system in a three-tray section of a cyclic absorber. Fluctuations in liquid-heads and interstage pressure differences; entrainment of small air bubbles in the downflowing liquid; and weepage of liquid due to liquid "sloshing" in the gas flow period have been found to have a pronounced effect upon column hydraulics.

17. Key Words and Document Analysis. 17a. Descriptors

Air Pollution
Absorbers (equipment)
Operations
Industrial Engineering
Cyclic Load
Axial Flow
Air Flow
Liquid Flow
Mixing
Steady State
Simulation
Head (fluid mechanics)

17b. Identifiers/Open-Ended Terms

17c. COSATI Field/Group 13B

18. Availability Statement: Unlimited	19. Security Class (This Report) UNCLASSIFIED	21. No. of Pages 76
	20. Security Class (This Page) UNCLASSIFIED	22. Price $3.00

FORM NTIS-35 (REV. 3-72)

THIS FORM MAY BE REPRODUCED

USCOMM-DC 14952-P72

EPA R-2-72-023

EPA-R2-72-023
May 1972

PB 211 853

CYCLIC OPERATION OF PLATE COLUMNS FOR GAS-LIQUID CONTACTING

by

James D. Dearth

Lawrence B. Evans

Edwin R. Gilliland

Department of Chemical Engineering

Massachusetts Institute of Technology

Cambridge, Massachusetts

May 1, 1972

Reproduced by
NATIONAL TECHNICAL
INFORMATION SERVICE
U S Department of Commerce
Springfield VA 22151

This report describes work carried out from October, 1971 through May, 1972 under Task Order No. 2 of EPA Contract 68-02-0018.

176

PREFACE

This report describes the results of work carried out under Task Order No. 2 of EPA Contract 68-02-0018. during the period October, 1970 through May, 1972. This work comprises doctoral thesis investigation of Mr. Dearth being carried out under the supervision of Professors Gilliland and Evans. When it is completed the results will be described in full in Mr. Dearth's doctoral thesis.

A decision has been made to seek continued support for completion of the work by means of an EPA grant rather than through extension of the current contract. This report, therefore, serves as an interim report to document the progress achieved to date under the contract and to support the proposal for a grant.

ABSTRACT

Previous experimental and theoretical work has indicated that the efficiency and capacity of gas-liquid contacting equipment may be improved by controlled-cycling of gas and liquid flows. However, difficulties encountered in the design of large-scale systems, where hydraulic instabilities and axial liquid mixing effects have been found to be severe, has prevented wide-scale application of such systems to industrial separations. This report describes a proposed program for obtaining needed information on tray hydraulics and liquid mixing, and summarizes some initial data and tentative conclusions for both steady-state and cyclic flows of an air-water system in a three-tray section of a cyclic absorber. Fluctuations in liquid-heads and interstage pressure differences; entrainment of small air bubbles in the downflowing liquid; and weepage of liquid due to liquid "sloshing" in the gas flow period have been found to have a pronounced effect upon column hydraulics.

CONTENTS

	Page
I. Introduction	
A. General Description and Motivation	1
B. Literature Review	2
C. Current Problem Areas	5
II. Objectives	
A. Short-range	7
1. Experimental	7
2. Computational	8
B. Long-range	8
III. Apparatus	10
IV. Experimental Approach	
A. Hydraulics	12
B. Liquid Mixing	15
V. Results and Tentative Conclusions	
A. Hydraulics	16
1. Steady-state Air Flow	16
2. Steady-state Liquid Flow	19
3. Variable-Venting Experiments	26
4. Vented Cyclic Results	30
5. Sealed Steady-State and Cyclic Operation	34
B. Liquid Mixing	36
C. Mathematical Simulation Models	37
1. Hydraulics	37
2. Mass-transfer Model with Mixing	40
VI. Direction of Current and Future Work	40
VII. Summary	42
VIII. Appendix	43

		Page
A.	Models for Axial Liquid Mixing in Cyclic Operation	43
	1. Liquid-Phase Mixing from Evolution of Vertical Concentration-Distance Profile.	43
	2. Overall Mixing Parameter from Measurements of Well-Mixed VFP Composition	45
B.	Model for Gas and Liquid Flows Through a Perforated Plate.	47
C.	Mathematical Model for Mass-Transfer and Liquid Mixing in a Cyclic Absorber.	51
	1. Gas Flow Period	51
	2. Plug-Flow Conditions	52
	3. Mixing-Model Equations	52
	4. Periodicity Conditions	53
	5. Average Exit-Gas Composition	53
	6. Overall Column Efficiency	54
	7. Dimensionless Form	54
D.	Sample Calculations	59
	1. Comparison of Experimental Slope of Liquid-head vs. Flow Rate with Hagen-Poiseuille Law.	59
	2. Calculation of Flowrate for Critical Weber Number.	60
	3. Effect of Liquid Aeration on Velocity-Head	60
	4. Initial Rate of Pressure Rise Due to Air Flow into a Sealed Column Section	61
	5. Estimate of Liquid Residence-Time and Ratio of Flow-Period Lengths.	61
E.	Nomenclature.	63
F.	Literature Cited.	69

I. Introduction

A. General Description and Motivation

Increased process efficiency and equipment capacity are among the benefits which can result from controlled cycling of many traditionally steady-state chemical engineering operations. Sufficient studies, both experimental and theoretical, have been conducted to demonstrate that benefits can accrue from imposing a repetitive discontinuity upon an otherwise continuous operation. Because of the widespread use of gas-liquid contacting equipment in industry for distillation or gas absorption applications, it is felt that the introduction of controlled cycling into this area may have a substantial impact upon the economics of any process which utilizes these unit operations for purification or product recovery. In particular, the perfection of a high-capacity, high-efficiency tail-gas scrubber design might help to reduce the economic burden imposed on many industries by the advent of stricter state and federal pollutant emissions standards.

This investigation is concerned with the design of staged gas-liquid contacting equipment for cycled operation. The configuration currently under consideration resembles a conventional sieve-tray column, but lacks the weirs and downcomers associated with normal crossflow operation. Each operating cycle consists of two distinct phase-flow periods. During the vapor flow period gas is allowed to flow upward for a short period of time, at a rate sufficient to maintain a

pool of liquid on each tray without leakage through the perforations. Mass transfer occurs across the interface between the rising gas bubbles and the vigorously agitated liquid. During the liquid flow period the gas flow is interrupted and liquid is allowed to drain through the trays by a weepage mechanism, while fresh liquid is fed into the column. Before proceeding to outline the objectives of the current study and the organization of the research program, it would be appropriate to review the historical development of controlled-cycling and to summarize some of the important conclusions of previous investigators.

B. Literature Review

The concept of cycled operation was originated by Cannon (1) in 1952. At that time it was suggested that many existing mass-transfer operations might be substantially improved by changing the method of contacting the flowing phases. The first mention of an operating cycle was made four years later in connection with a proposed liquid-extraction process which employed alternate upflow and downflow of the light and heavy phases (2). Cycled or "pulsed" columns of this type were found to have high separation efficiencies and capacities, and many have since found their way into industrial use. Other cycled systems have been employed on a laboratory scale for particle-size segregation, crystallization, and ion exchange (16, 12, 20).

The first data on cycled gas-liquid systems were reported by Gaska and Cannon (5) and McWhirter and Cannon (13) for the

rectification of benzene-toluene and methylcyclohexane-n-heptane mixtures in a 2-inch ID glass column. It was concluded from these early investigations that cycled distillation columns could be operated for either high efficiency or high capacity, depending upon the relative lengths of the gas and liquid flow periods. The highest column efficiencies observed were in the range 130 to 150%, indicating that each tray of a cycled column had a separating ability superior to that of a single "theoretical plate." In a subsequent investigation McWhirter and Lloyd (14) confirmed the earlier results using a 6-inch ID column containing five 3-inch "packed plates." For operating cycles of 3 to 9 seconds' duration overall efficiencies were in the range 160 to 200%. The observed separating ability was rationalized in terms of the greater average mass-transfer driving forces present in a cycled column. A simple mathematical model of a cycled column confirmed this hypothesis and predicted efficiences similar to those observed.

Theoretical analyses by Robinson and Engel (17) and Sommerfeld, et al. (19) established an exact analogy between the time-axis concentration profiles in a cycled column and the crossflow concentration gradients in conventional columns. The latter case had been analyzed by Lewis (9) who concluded that such gradients could produce substantial improvements in the efficiency of bubble-cap trays. Analytical transient solutions to McWhirter's model were developed by Chien, et al. (3) for the simplest case of a linear equilibrium relation, and iterative procedures were developed to handle more general non-

linear expressions. An extensive simulation study was carried out to determine the effects of local point efficiency, slopes of the operating and equilibrium lines, amount of liquid dropped during the liquid flow period, and other parameters, on both overall column and individual plate efficiencies. The most important conclusions may be summarized as follows:

1) For controlled cycling operation at total reflux with negligible liquid mixing during the liquid flow period, the overall column efficiency attains its maximum value when the contents of one tray are dropped per cycle.

2) Liquid mixing during the liquid flow period tends to degrade the efficiency improvement obtained by cycling. In the limit of perfect mixing there is no improvement.

3) The fractional increase of column efficiency between noncycled and cycled operation is greatest when the individual point efficiencies are high.

4) The overall column efficiency increases to an asymptotic limit as the total number of stages is increased. This limiting behavior of overall efficiency was noted by Horn (8), who developed an asymptotic solution using z-transform techniques.

Schrodt, et al. (18) carried out a series of experiments using a 12-inch ID cycled column containing 15 perforated trays without downcomers. It was concluded that the cyclic unit was superior in flexibility and throughput characteristics to the same unit in conventional dual-flow operation; however, the cycled column efficiencies were, at best, slightly lower than for conventional-flow. One reason for this was that the column operation was hydrodynamically unstable. It was noted that the existence of dynamic flow lags often caused the lower trays to drain completely before the liquid had begun to flow from the upper trays. Gerster and Scull (6), in studying the cyclic desorption of ammonia from aqueous solu-

tion into an air stream, observed a different type of instability in the form of excessive liquid accumulations on the lower trays. Despite unimpeded liquid mixing, efficiencies as much as 40 percent higher than those obtainable in conventional service were reported. A model for liquid mixing was proposed and incorporated into the existing model for mass transfer. The data were found to be in good agreement with the model predictions, and values of a single "mixing parameter" were estimated.

To gain insight into the nature of the hydraulics of a cycled column Wade, et al. (21) formulated a reasonably detailed mathematical model of a cycled distillation column. Using several empirical relations for gas and liquid flow rates, they found that it was possible to alleviate the problem of liquid-flow lags by strategic manipulation of isolation valves in the lines to the condenser and reboiler. The shortcomings of the model and of the method of solution were as follows:

1) The hydraulic relations used were completely empirical, with no experimental justification.

2) The solutions obtained were for single cycles or small numbers of cycles. No attempt was made to select initial conditions to satisfy the periodicity conditions of pseudo-steady cycled operation.

3) For convenience in the solution of the model equations, perfect mixing of the liquid phase was assumed at all times.

C. Current Problem Areas

Thus far, a general lack of understanding of the tray hydraulics and liquid-mixing phenomena which occur in full

scale cyclic equipment has made it virtually impossible to apply the results obtained from simulation studies to the design of multistage cyclic cascades. In the first place, the existing models for cyclic mass-transfer presuppose a knowledge of the liquid holdup on each tray. This quantity is determined by the liquid head needed to drive a specified flow rate of liquid down through the tray perforations against an opposing gas-phase pressure difference. This flow configuration has received little attention in previous literature, since in a conventional crossflow tray weepage of liquid through the holes is undesirable: in fact, much effort has been directed towards the prediction of the minimum gas velocities needed to prevent liquid flow through the holes. Existing theories are unable to predict the magnitudes of liquid heads and gas-phase pressure differences, and the phenomenon of free liquid drainage with no gas-phase pressure difference appears not to be adequately described by simple orifice equations. Yet liquid holdup is a predominant factor in determining point contacting efficiency and cycle time.

There is additional experimental evidence which indicates that hydraulic coupling among successive stages may result in undesirable drainage-rate and holdup characteristics. Trays near the top end of the column may run dry while excessive amounts of liquid may accumulate on the lower trays. Qualitative explanations for these phenomena have been suggested, but no quantitative techniques have been developed to predict the occurrence of hydraulic instabilities and to indicate

methods for alleviating their undesirable effects upon column performance by proper design.

The results of a ground-breaking study of axial liquid mixing have suggested an effective one-parameter mixing model which can be easily incorporated into the existing overall simulation scheme for cyclic absorption. It remains to correlate the extent of mixing against flowrates, liquid heads, and geometric parameters in order to indicate column design configurations for minimizing the undesirable effects of liquid mixing during the LFP.

II. Objectives

A. Short-Range.

The purpose of the current research program is to provide information necessary to the formulation of rational criteria for the design of cyclic absorbers. The immediate objectives of such a study are summarized below.

1. Experimental.

The goal of the experimental phase of the work is to provide information on the physical processes which influence the hydraulic operation of cyclic columns. Once the important phenomena are understood, the data obtained can be used to test mathematical models and evaluate parameters in the proposed correlations. The specific objectives are as follows:

a. To develop correlations for predicting gas and liquid flows as functions of liquid

head and interstage pressure difference, for various tray geometries.

b. To evaluate alternative column configurations and modes of operation to gain an appreciation of their relative advantages and limitations.

c. To evaluate mixing parameters and correlate them to hydraulic and geometric variables.

2. Computational.

The shortcomings of previous attmpts to simulate hydraulics and mass-transfer under controlled-cyclic conditions were due primarily to the lack of experimental hydraulic data. It is anticipated that this need will be adequately filled by the correlations derived from the experimental phase of the work, and that the following simulation studies may then be carried out:

a. To simulate the hydraulic behavior of a long cyclic cascade, noting any non-uniformities of flow or liquid-head distribution predicted.

b. To simulate the overall mass-transfer behavior of a cyclic absorber, to obtain values of overall column efficiency as functions of a set of column parameters specified by the designer.

B. Long-range.

The ultimate objective of the research program is to

answer the following set of design questions:

1. Is cyclic operation of absorption and distillation systems technically feasible?
2. What are the optimal choices for the design and operating parameters?
3. Is the "best" cyclic system economically competitive with existing equipment?

The studies carried out to date seem already to have answered the first question in the affirmative. It remains to solve the optimal design problem and to interpret the results in the light of similar experience for conventional columns.

The design model formulated in the initial stages of the research program should be tested against experimental results to assess its reliability. A reasonable method for carrying out such tests is to select a gas-liquid system and to conduct a series of small-scale experiments to develop correlations for point efficiency. The efficiency correlations, together with equilibrium data and specifications of inlet and outlet gas concentrations and gas flow rate, are fed into the mathematical model, and an optimum set of design-variable values is generated. The actual performance of this "optimal" column once constructed may then be compared with that predicted by the model. The results of such a study would yield information on both the shortcomings of the model and the actual separations obtainable in a well-designed cyclic absorber.

III. Apparatus.

The experimental apparatus shown in Figure 1 consists of a three tray section of a 6-inch diameter Lucite column, with associated gas and liquid supply systems. The trays are fabricated from 1/4-inch thick plexiglas sheet with holes drilled on a triangular pitch. A sightglass is provided on each of the bottom two trays for measurement of the average clear liquid head, and a manometer is provided for measurement of the interstage pressure difference across each of the test trays. The tray inserts currently in use contain 1/8-inch holes, with a fractional perforated area of 10%. In order to insure uniform drainage, the bottom of each tray is sprayed with a fluorinated hydrocarbon coating to make it non-wettable.

The gas used is air, supplied from a 125 psig oil-free compressed air line, passed through a reducing pressure regulator, humidified to 95% of saturation, and delivered to the base of the column through 1-inch supply lines containing orifice plates for flow metering. The liquid phases consist of water and a dilute sodium chloride tracer solution pumped from two identical 150-gallon polyethylene tanks through a set of rotameters to the top of the column.

Cyclic control of flows is imposed by placing 3-way solenoid valves in the lines, in close proximity to the column. During their respective "off"-cycles the air will be vented, while water and tracer solution will be returned to their storage tanks. This arrangement permits continuous metering of flows even under conditions of cyclic operation. The sole-

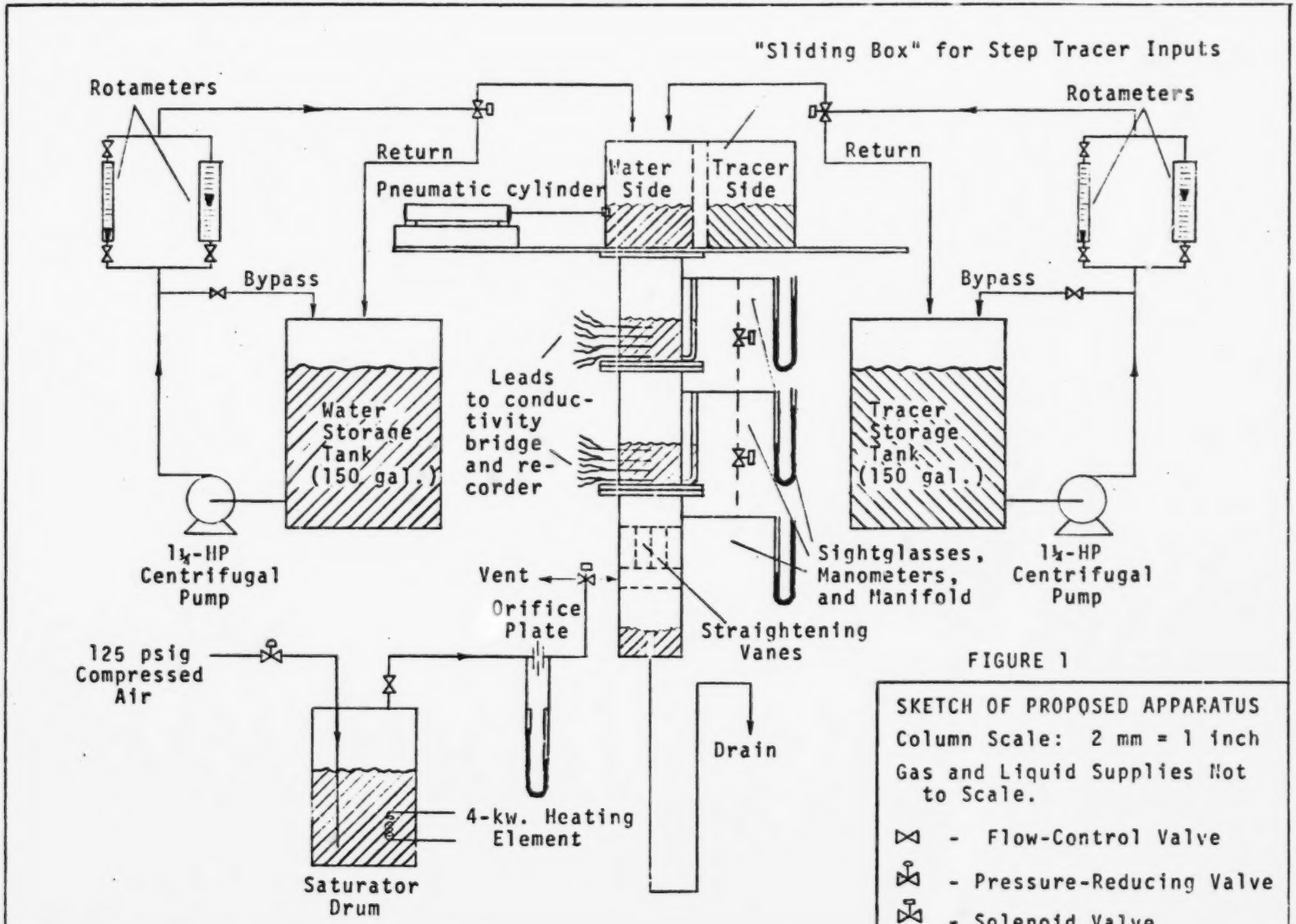

FIGURE 1

SKETCH OF PROPOSED APPARATUS
Column Scale: 2 mm = 1 inch
Gas and Liquid Supplies Not to Scale.

⋈ - Flow-Control Valve

⋈ - Pressure-Reducing Valve

⋈ - Solenoid Valve

(JDD 11/15/70)

noid valves are operated by electrical signals from a cycle-timer-relay control box, which permits independent variation of the gas and liquid flow period lengths.

To permit optional venting of the column sections to atmospheric pressure, a set of solenoid valves is mounted at the rear of the frame. Each valve is connected to a venting port in a particular column section, and may be closed or opened by manual switching or by cyclic relay control. A float valve has been installed in the bottom of the column to seal the liquid drain line and prevent the oscillations in the overflow leg during the gas flow period.

A rather unique feature of the apparatus is the "sliding box" arrangement provided for the alternate introduction of water and salt solution during liquid-mixing experiments. The box has two chambers, one containing water and the other, tracer solution. The position of the box relative to the perforations in the top plate is controlled by the piston of a pneumatic cylinder, so situated that either chamber may be located above the column. Salt concentrations in the liquid on a particular tray may be monitored by inserting 5 mm. glass conductivity probes through the side wall of the column. Fittings allow the probes to be traversed radially in order to check for concentration gradients in the radial direction.

IV. Experimental Approach.

A. Hydraulics.

In dealing with the complex phenomena associated with the hydraulics of a sealed cyclic column, it has been found advantageous to decompose the more difficult general

problem into a sequence of individual sub-problems more amenable to measurement and interpretation. The piece-wise - steady nature of cyclic operation suggests that one might reasonably group the phenomena of interest into three main subdivisions as follows:

1. Steady-state gas flow through a non-flowing mass of aerated liquid supported on a sieve tray.
2. Steady-state liquid drainage through the perforations of a sieve tray against an opposing gas-phase pressure difference.
3. Departures from steady-state gas flow and liquid drainage, resulting from on-off flow cycling.

Each of these sub-areas can, in turn, be broken down into their component phenomena, as illustrated by the diagram in Figure 2. Pressure drops for gas flow are, in general, represented as the sum of a dry-plate component and a liquid-head contribution. In an analogous fashion, steady-state liquid heads can be thought of as being composed of a liquid head for free drainage with no gas-phase pressure difference, and an additional level difference to overcome the effect of pressure buildup in the gas phase. Similarly, the departures from steady-state hydraulics may result both from phenomena which arise when the column sections are vented during the liquid flow period, and from other effects due exclusively to the decay of the pressure gradient set up during the vapor flow period.

The independent variables and their approximate ranges of variation may be summarized as follows:

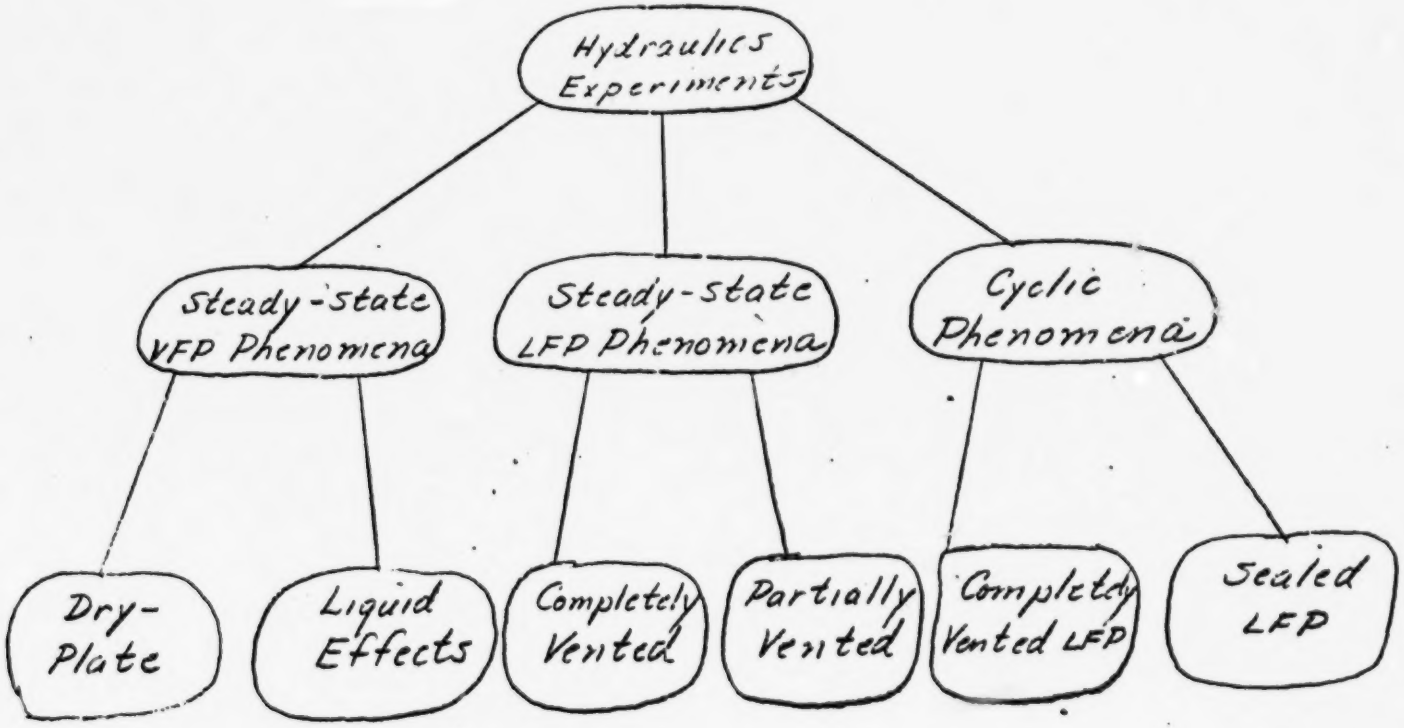

Breakdown of
Hydraulic Phenomena

FIGURE 2

1. Gas Flow Rate: 0.5 - 1.5 ft^3/sec (1 atm, 70°F)
2. Liquid Flow Rate: 1 - 30 gal/min.
3. Gas Flow Period: 0.5 - 10 sec.
4. Liquid Flow Period: 0.5 - 10 sec.
5. Tray Hole Diameter: 1/8 - 1/2 inch
6. Tray Free Area: 5 - 20 %

B. Liquid Mixing.

The values of liquid mixing parameters reported in the literature have been deduced from mass-transfer experiments by comparing the experimental results with those obtained from the mathematical simulations modified to include a simple mixing model. The excellent agreement reported between theory and experiment for a constant mixing parameter value is an encouraging sign that the model selected may give a good representation of the actual column behavior.

What is now needed is a correlation of mixing-parameter values as functions of liquid flow rate, liquid holdup, plate spacing, and tray geometry. For this purpose, mass-transfer experiments would be both expensive and time-consuming, and the results might contain errors and uncertainties due to imperfect modelling of mass-transfer phenomena and inaccurate values of input parameters such as point efficiency. As an alternative it has been found desirable to devise a means to test the mixing model in the absence of mass-transfer, thus taking advantage of the fact that mixing of liquid on the trays results only from hydraulic phenomena.

The experimental technique involves the introduction into the test column of water and a dilute sodium chloride tracer solution during alternate liquid flow periods of cyclic operation. This alternating step-function concentration input gives rise to salt-concentration gradients in the vertical direction on each of the lower two test trays during the liquid flow period, as well as to up-and-down fluctuations in average tray liquid composition in alternate cycles. The distance-gradients and time-varying fluctuations in average concentration can be monitored by inserting conductivity probes into the tray liquid and recording the changes in the voltage imbalance of a bridge circuit which result from changes in the resistance of the solution. The distance-gradient results can be used to provide information on the detailed mixing process, while the average-concentration measurements permit the straightforward evaluation of an overall parameter. The interpretation of the results is discussed in Appendix VIII.A.

V. Results and Tentative Conclusions.

A. Hydraulics.

In the following sections, the results for gas and liquid flows through a 1/8-inch hole size, 10% free area tray insert have been summarized. Tentative conclusions, based on the existing information, have been formulated, and suggestions for further study in each of several areas have been made.

1. Steady-State Air Flow.

One of the first experiments performed on the completed column assembly was the measurement of dry-plate pressure drops for the first set of tray inserts. A large quantity of experimental data in this area is available in the literature and a general correlation of the data has been suggested by McAllister et al.(11). The usual approach is to express the pressure drop as a multiple of the velocity-head of the gas flowing through the holes. The proportionality constant which will be referred to as a "discharge-loss coefficient," is assumed to be equal to the product of a term representing the sum of sudden contraction losses, sudden expansion losses, and friction losses,multiplied by a function of the plate thickness to hole diameter ratio. A comparison of the data with this calculation is shown in Figure 3. The results have been plotted as discharge-loss coefficient vs. Reynolds number. The calculated value of the coefficient, neglecting the friction term, is 1.15. This is in excellent agreement with the data at the high-Reynolds number asymptote. At Reynolds' numbers below about 3000 the omitted friction-loss term seems to become important, resulting in an increase in the experimental coefficient. The scatter in the data at the low Reynolds' number end is due to the fact that in this region both gas flowrates and pressure-drops were extremely small, resulting in large percentage errors.

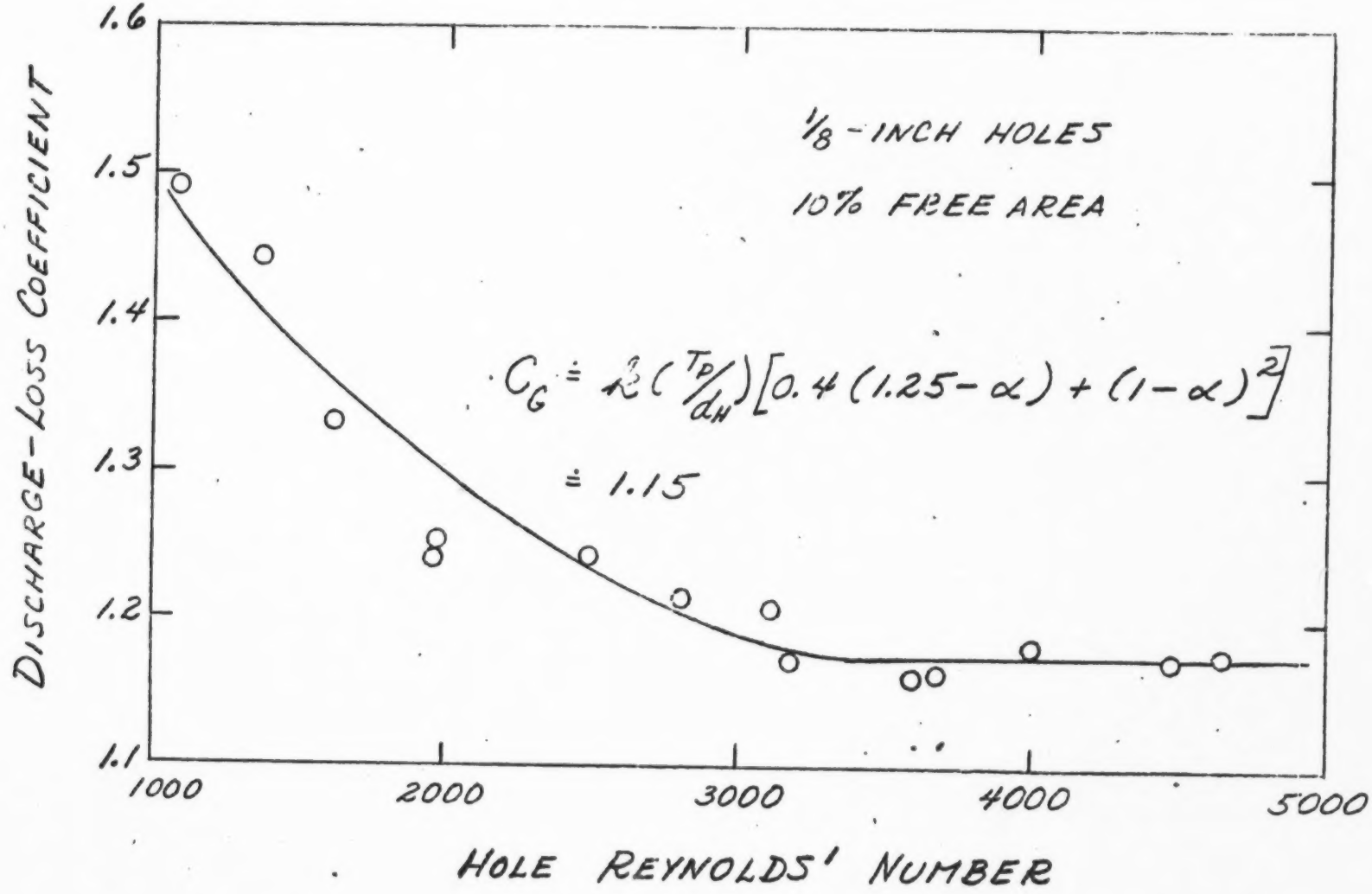
1/8 - INCH HOLES
10% FREE AREA
$C_G \doteq 2\left(T_D/d_H\right)\left[0.4(1.25-\alpha)+(1-\alpha)^2\right]$
$\doteq 1.15$
DISCHARGE-LOSS COEFFICIENT
1.6
1.5
1.4
1.3
1.2
1.1
1000
2000
3000
4000
5000
HOLE REYNOLDS' NUMBER

FIGURE 3

All experimental observations of cyclic operation to date suggest that, with one possible exception, transients at the beginning of the gas flow period are very fast. A fraction of a second after resumption of gas flow, the column is hydraulically at steady-state, and this steady-state is, for all practical purposes identical to that which one finds in a crossflow tray in the limit of zero liquid rate. Hence, one may make use of all available correlations for calculating wet-plate pressure drops from liquid heads and dry-plate pressure drops. If the liquid holdup on every plate is known at the end of the liquid flow period, the pressure gradient through the column during the gas flow period may be simply and efficiently computed. The modelling difficulties are associated almost entirely with liquid flow.

2. Steady-state Liquid Flow.

Two limiting modes of operation are of particular interest, when one considers the relationships governing liquid flow in a cyclic column. In the first case, henceforth referred to as "vented" operation, the intertray spaces are connected via electric or pneumatic valves to a common manifold. At the beginning of the liquid flow period these valves are opened, permitting essentially instantaneous equalization of gas-phase pressure across every tray. As a result, liquid flow is influenced only by the tray liquid head; no pressure buildups or fluctuations

may occur in the gas phase. The opposite extreme of "unvented" operation dispenses with the additional valves and manifold and allows interstage pressure differences to "seek their own levels." Pressures remain at non-zero values even after the inflow of air at the bottom is interrupted, and oscillations in the gas phase may have a significant effect upon liquid drainage. All stages are coupled together through the gas phase, and a disturbance in liquid head will be communicated up and down the column by resulting pressure disturbances.

A mathematical representation of either of these cases must make use of the fundamental steady-state discharge relationship for liquid flow through a perforated plate. This relationship is determined by means of the following experiment:

> With the pressure in all column sections maintained at one atmosphere, water is introduced through a distributor pipe at the top of the column at a specific volume flowrate. The liquid drains through the perforations of each plate and falls through the intertray space onto the tray below. Liquid heads are established on the various stages and are measured, with respect to some horizontal datum plane, on sightglasses.

The results are plotted as clear liquid head above datum in inches of H_2O vs. liquid volume flowrate in gallons per minute. Such a plot is shown in Figure 4 for the 1/8-inch hole size, 10% free area tray insert.

Although the data could be easily replotted as discharge-loss coefficient vs. Reynolds number, in analogy with the air-flow results, we will be content

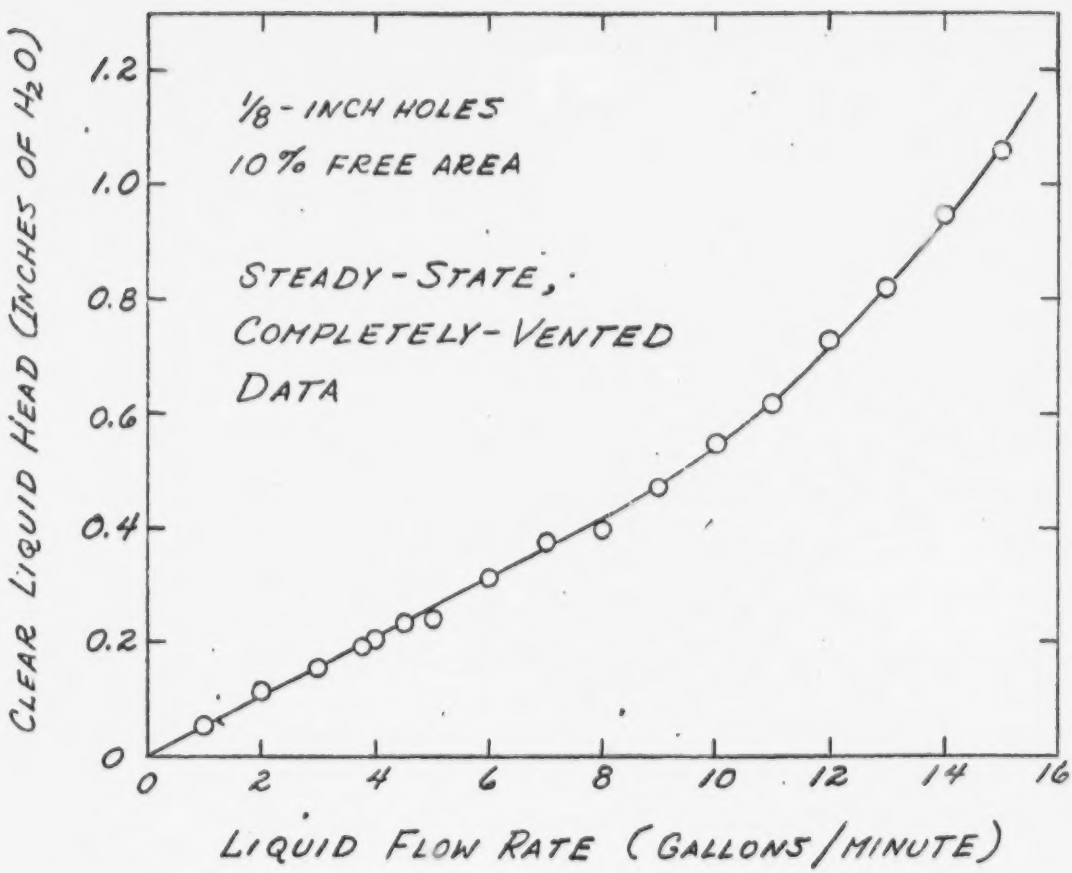
CLEAR LIQUID HEAD (INCHES OF H_2O)
1.2
1.0
0.8
0.6
0.4
0.2
0
1/8 - INCH HOLES
10 % FREE AREA
STEADY - STATE,
COMPLETELY - VENTED
DATA
0
2
4
6
8
10
12
14
16
LIQUID FLOW RATE (GALLONS / MINUTE)

FIGURE 4

for the moment with this simple representation. Note that at low flowrates the dependence is essentially linear and that at flowrates above about 10 gallons per minute the curve becomes concave upwards.

All flowrates in the range of experimental measurements correspond to Reynolds' numbers less than 2100, but because the entrance length required for complete development of a parabolic velocity profile is from one to two orders of magnitude larger than the length of each short tube, the discharge characteristics are dominated by entrance effects. A simple calculation (Appendix VIII.D.1) illustrates that the slope of the linear portion of the experimental curve is about 20 times what one would predict using Poiseuille's law. The predominant effects are the contraction of the entering jet and the shear of the tube wall. A discharge-loss coefficient defined for this case would be expected to have a value in the range 1.5 to 2.7, with a weak inverse power-dependence on Reynolds' number. This agrees well with the data at the high-flowrate end of the curve.

If there is no wetting of the bottom of the tray, liquid will drain as single drops until the inertia of the liquid flowing through the holes is sufficient to distort the dron shape and produce an elongated jet. The critical Weber number for this drop to jet transition is about 6.8. For the tray insert under consideration, this critical value corresponds to a

volume flowrate of 11.3 gallons/minute.(Appendix VIII.D.2.)

Above this flowrate jets have been observed to form at all holes; however, intermittent jetting has also been observed at flowrates considerably below this critical value. This seems to imply that local hole velocities may be large enough to give rise to jet formation, even though the average velocity, based on the entire perforated area, is not. In effect, we are saying that at any given time, only a fraction of the available holes is passing liquid. The data seem to indicate that this effective fraction increases as flowrate is increased, thus tending to moderate changes in the velocity head, and yielding the nearly-linear dependence observed at low flowrates. The sealing and unsealing of holes is believed to be brought about by the fluctuations of liquid head at various locations on the tray, with liquid flow occurring at those perforations where the instantaneous local liquid head is sufficient to overcome surface tension.

A further complication results from the fact that liquid drops or streams falling onto a free liquid surface entrain air bubbles into the bulk liquid phase. Some of these pass on through the perforations with the downflowing liquid and enter the gas space below. This phenomenon produces a small steady flow of the gas phase down the column

during the liquid flow period.

If there is good disengagement of gas from liquid in the bottom of the column, then in the completely vented mode all air that passes down through the bottom stage by this entrainment mechanism must exit through the bottom venting port. Hence, to measure the rate of air entrainment one needs to measure only the flow rate of air through the vent. Since rotameters and soap-film meters were found to be unsatisfactory flow-measuring devices due to excessive pressure drops, a scheme was devised for mixing a small metered flowrate of CO_2 with the main vent air stream. The air flowrate was calculated from the known CO_2 rate and the mole fraction of CO_2 in the mixture, determined chromatographically. The results are shown in Figure 5.

This plot shows air entrainment rate in cc./sec. as a function of liquid flowrate in both gallons/minute and cc./sec. The curve is seen to be "s"-shaped, with an apparent point of inflection in the vicinity of 8 gallons/minute. The interpretation of such data is quite complicated, since at least two competing processes are at work. Increasing the liquid flowrate by itself probably tends to increase the entrainment rate by increasing the total volume of air bubbles in the liquid phase, as well as by increasing the size of the largest bubble whose terminal rise velocity will be exceeded. On the other hand, the accompanying increase in liquid holdup makes it

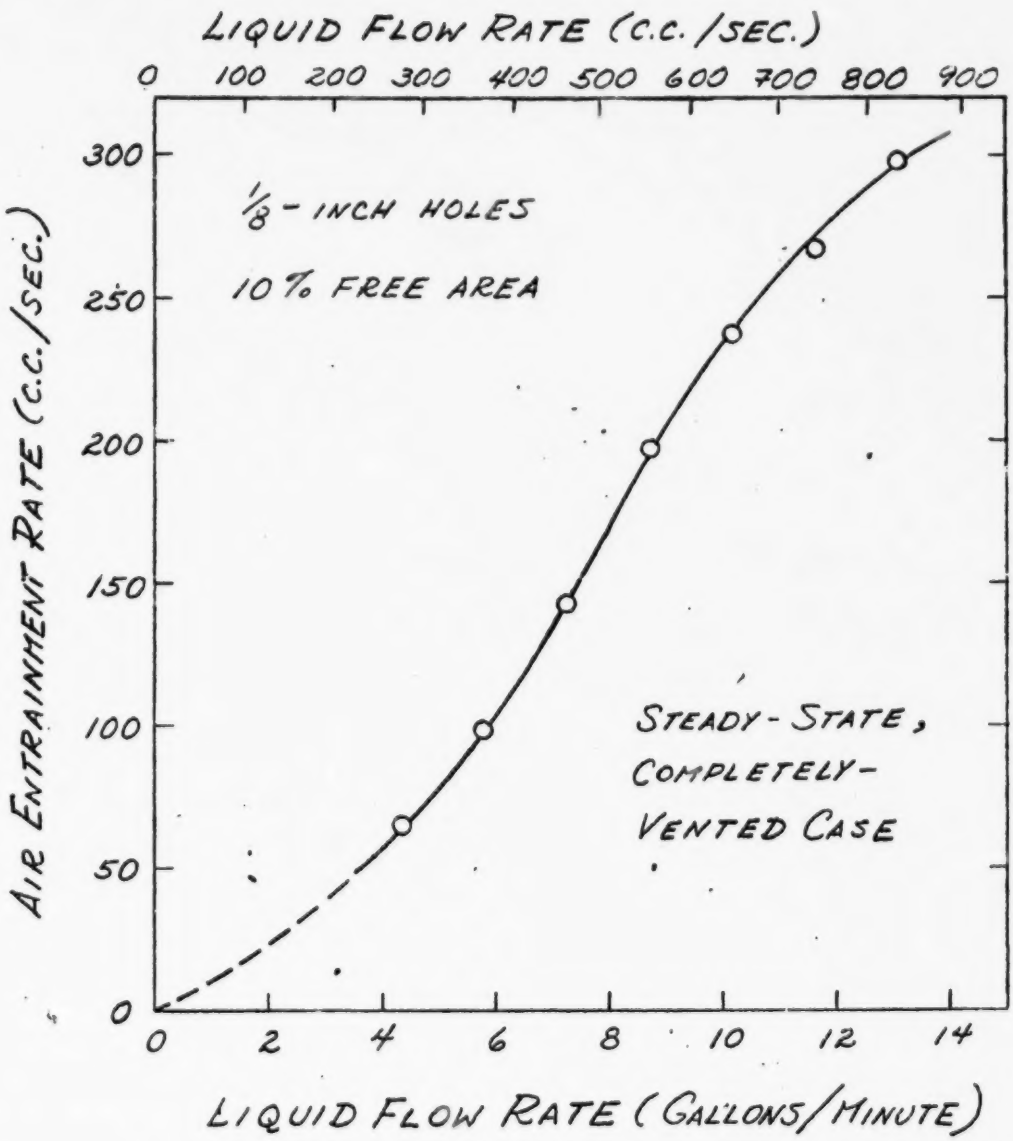
LIQUID FLOW RATE (C.C./SEC.)
0
100
200
300
400
500
600
700
800
900
AIR ENTRAINMENT RATE (C.C./SEC.)
300
250
200
150
100
50
0
1/8 - INCH HOLES
10 % FREE AREA
STEADY - STATE,
COMPLETELY -
VENTED CASE
0
2
4
6
8
10
12
14
LIQUID FLOW RATE (GALLONS/MINUTE)

FIGURE 5

more difficult for bubbles to penetrate to the tray surface. The latter effect is more important at high flowrates and probably accounts for the decreasing slope at the upper end of the curve. These data indicate a 20 to 30 percent aeration of the liquid flowing down through the holes. If the mixture of air and water is a uniform froth of small bubbles in the liquid it can be shown (Appendix VIII. D.3.) that the pressure drop for flow through the perforations is from 30 to 40 percent larger than for the same volume rate of non-aerated liquid.

3. Variable-venting Experiments.

Another simple calculation (Appendix VIII.D.4) shows that pumping air at a rate of 200 cc./sec. into a sealed volume of 5.5 liters maintained at room temperature results in an initial rate of pressure change of 1 inch of water every 0.07 second. Thus, the hydraulic consequences of air entrainment can be quite significant in an unvented column. One can imagine an experiment in which the bottom vent line is gradually closed. If air is carried down by the liquid into this closed gas space the pressure increases, the liquid head builds up, and as a result, the rate of influx of air is diminished. At steady-state the flowrate of air into the sealed section must be balanced by an equivalent outflow, either by entrainment of small bubbles in the exit stream or by air bubbling up through the perforations.

Such variable-venting experiments have been car-

ried out by adjusting a valve in the vent line from the bottom section. Figures 6 and 7 show the effect upon tray liquid head and interstage pressure difference of decreasing the air venting rate from its maximum value to zero. Pressure difference and clear liquid head in inches of water have been plotted against air venting rate in cc./sec., for a range of different liquid flow rates. When the vent valve is fully-open the pressure difference is zero and the liquid-head lies on an envelope corresponding to the "s" shaped entrainment curve discussed previously. As the venting rate is reduced to zero the pressure difference and liquid head increase, gradually at first, with a final sharp rise as the venting rate is decreased below about 15 cc./sec.

The difference between the clear liquid head and the differential pressure constitutes a net pressure difference favoring liquid flow. In Figure 8 values of this quantity are plotted against air venting rate. These data indicated that at a fixed liquid flowrate the net difference decreases as the vent is closed, even though the individual values of liquid head and gas-phase pressure difference are increasing. In effect, this says that it is "easier" to force a given flowrate of liquid down through a tray into a sealed vapor space than into a vented space, whereas one would intuitively expect that the net difference of head should be about the same in both

Reproduced from best available copy.

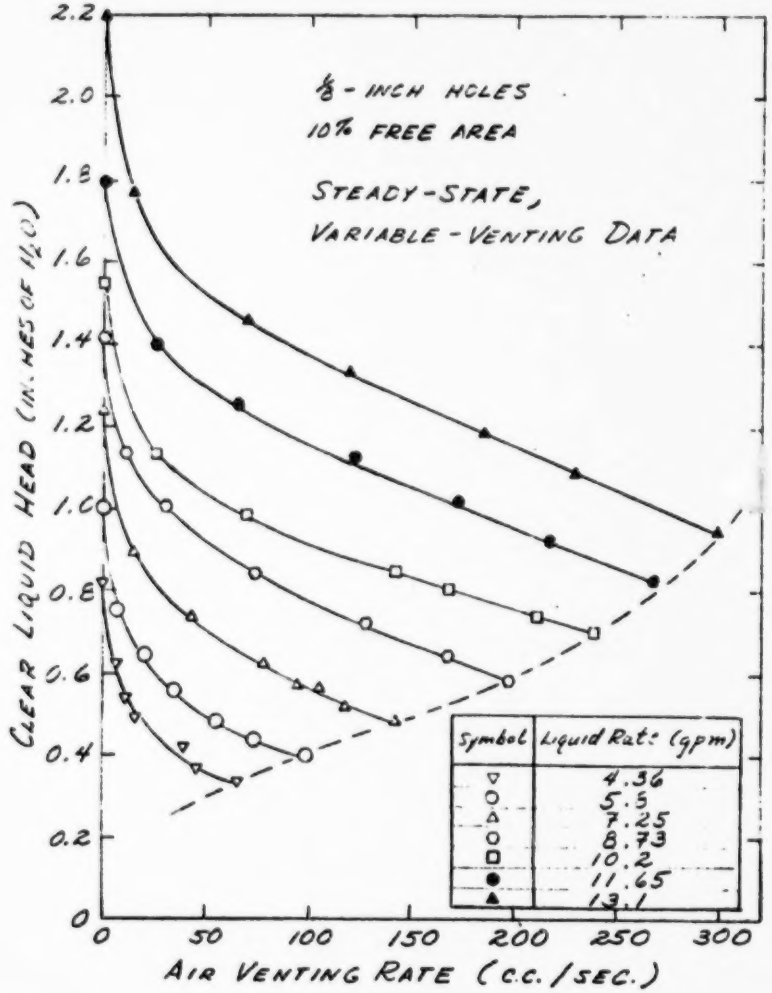

FIGURE 6

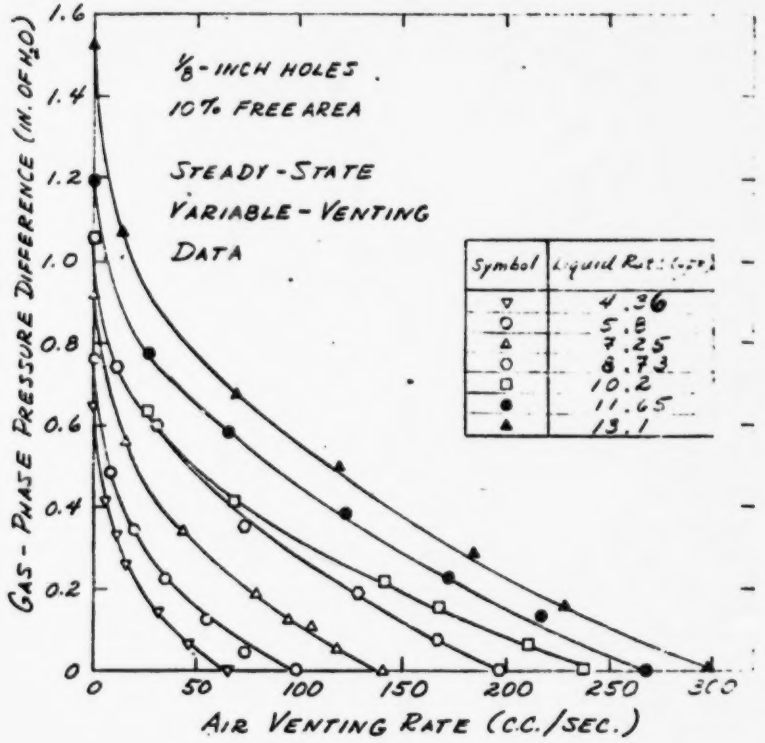

FIGURE 7

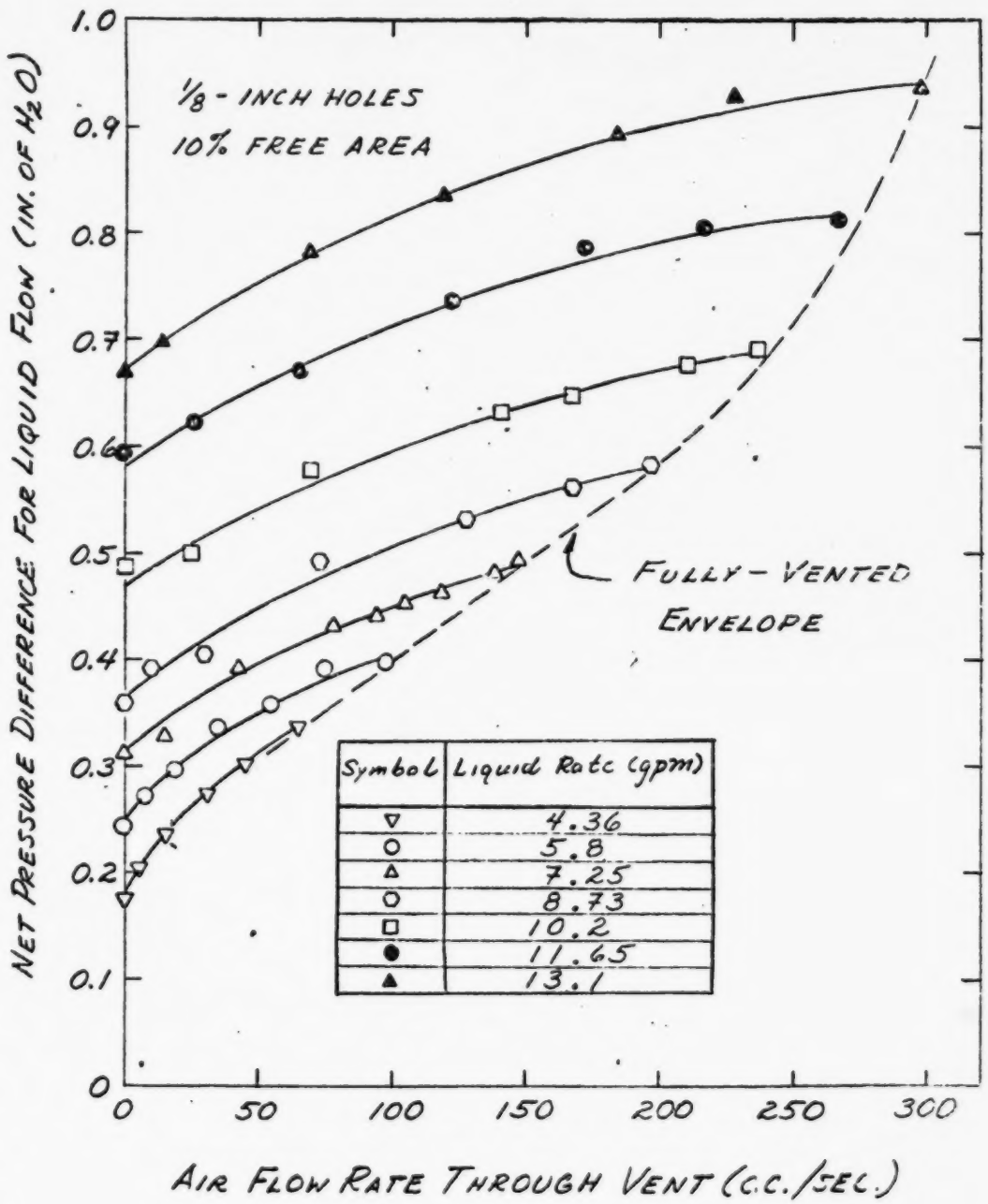
1.0
0.9
0.8
0.7
0.6
0.5
0.4
0.3
0.2
0.1
0
0
50
100
150
200
250
300
1/8 - INCH HOLES
10% FREE AREA
FULLY - VENTED
ENVELOPE
Symbol | Liquid Rate (gpm)
4.36
5.8
7.25
8.73
10.2
11.65
13.1
NET PRESSURE DIFFERENCE FOR LIQUID FLOW (IN. OF H2O)
AIR FLOW RATE THROUGH VENT (C.C./SEC.)

FIGURE 8

cases.

Two factors seem to be at work here. First, as the vent valve is closed and liquid head is allowed to build up, the fraction of air bubbles in the liquid draining through the holes is cut down dramatically. As pointed out earlier, decreasing air entrainment decreases the velocity-head of the flowing gas-in-liquid dispersion, so that one might expect to observe a drop in the required pressure difference. Second, when the column section is sealed, pressure fluctuations in the gas phase increase in magnitude. It can be shown that such fluctuations act to overcome the stabilizing influence of surface tension, and allow larger flow rates of liquid with the same average net pressure difference. More air-entrainment data are needed at different flowrates and liquid heads in order to draw quantitative conclusions about the relative importance of these factors (Appendix VIII.B.). It is anticipated that experiments with different tray inserts will provide the necessary information.

4. Vented Cyclic Results.

One of the reasons for investigating the clear liquid head vs. liquid flow relationship at steady-state was that the results were expected to be applicable to a vented cyclic column. It was hoped that the removal of gas-phase pressure differences would stabilize liquid flow, so that liquid holdups would

be about the same on all stages and equal to the values predicted from steady-state data. In fact, although the expected stabilization of flow was achieved, clear liquid heads measured in controlled-cyclic operation were found to be consistently lower than those measured at steady-state. A comparison of results for the two cases is shown in Figure 9. The plot shows clear liquid head in inches of water as a function of liquid flow rate in gallons per minute. The solid circles denote steady-state results, while the open symbols represent cyclic data at various liquid flow period lengths, ranging from 1.2 to 9.6 seconds. The gas flow period and air flow rate were held constant at 5.4 seconds and .9 $ft^3/sec.$, respectively.

The clear liquid heads measured for the cyclic case are observed to be always less than the corresponding values at steady-state, regardless of liquid flow rate or length of liquid flow period. The effect of liquid flow period length is most pronounced at the high liquid rates where the shorter liquid flow periods give rise to smaller clear liquid heads. The near-coincidence of the curves for liquid flow periods of 5.4,7.8, and 9.6 seconds seems to indicate that as LFP length is increased indefinitely an asymptotic upper limiting liquid head is approached at a given flowrate.

There is good evidence to support the contention that weepage during the vapor flow period may be part-

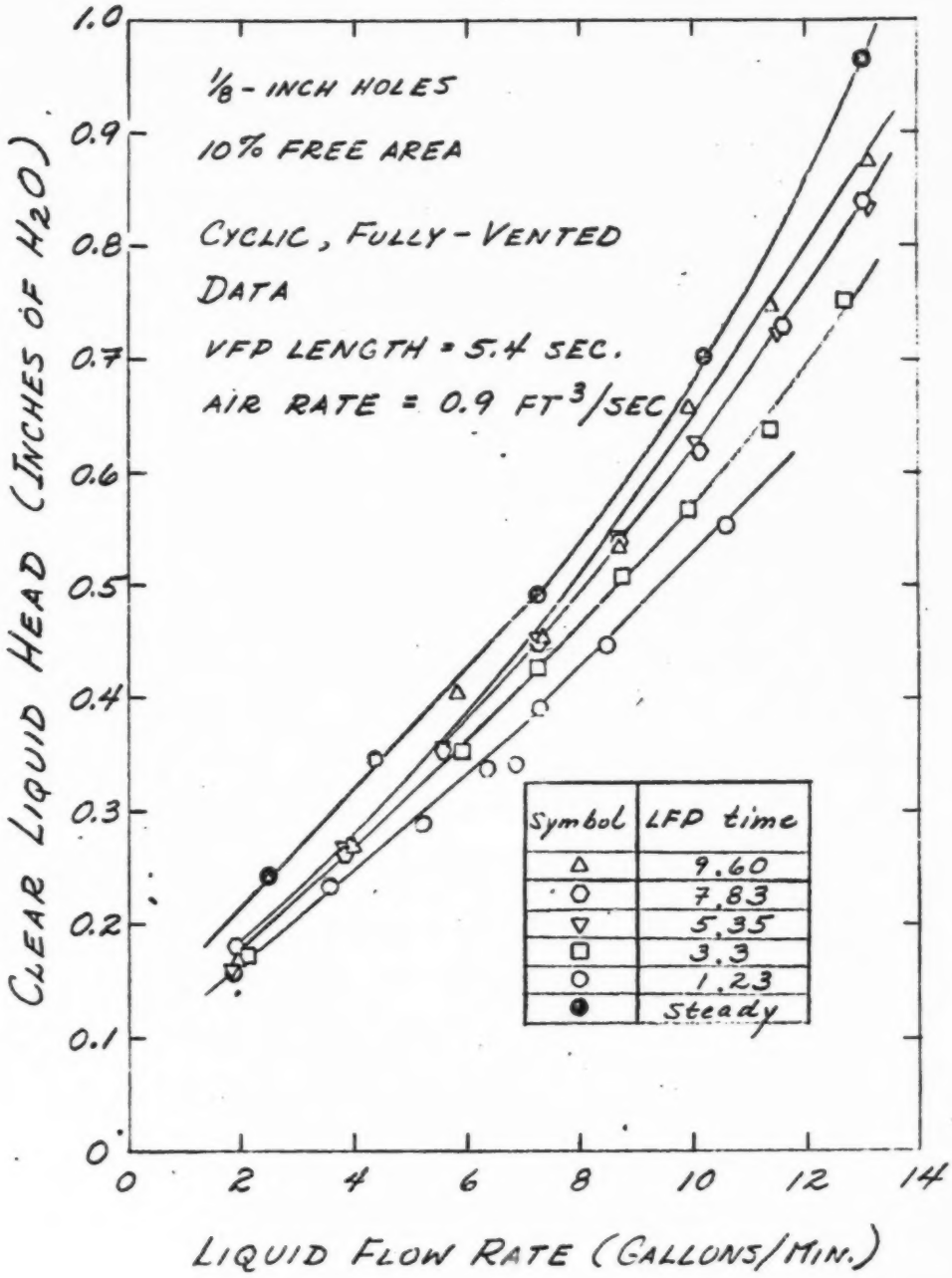
1/8 - INCH HOLES
10% FREE AREA
CYCLIC, FULLY-VENTED
DATA
VFD LENGTH = 5.4 SEC.
AIR RATE = 0.9 FT³/SEC
Symbol | LFD time
△ | 9.60
○ | 7.83
▽ | 5.35
□ | 3.3
○ | 1.23
● | steady
CLEAR LIQUID HEAD (INCHES OF H2O)
LIQUID FLOW RATE (GALLONS/MIN.)
0
0.1
0.2
0.3
0.4
0.5
0.6
0.7
0.8
0.9
1.0
0
2
4
6
8
10
12
14

FIGURE 9

ly responsible for the observed discrepancies. Gradual shifts in the sightglass levels have been noted during the course of a cycle, indicating a decrease of liquid level during the vapor flow period. At large holdups or gas flowrates a side to side oscillation of the froth has been found to produce brief spurts of liquid flow near the side walls. If liquid flow occurs during part of the VFP, the actual flowrate per unit time will be reduced from the value obtained by assuming flow only in the LFP, and this reduction in average flowrate will be reflected in a smaller value of clear liquid head. Since the total liquid weepage per cycle is equal to the average weep rate multiplied by the gas flow period length, the correction for weepage is largest when the VFP/LFP ratio is large, and it is under these conditions that the maximum discrepancies in liquid holdup are observed. However, the weepage hypothesis does not seem to account for the differences between the cyclic and steady-state results at low flowrates.

At present time experiments are being undertaken to measure the effect of varying LFP time, VFP time, and the VFP/LFP ratio, in order to determine the extent of their interactions. It would also be instructive to eliminate liquid oscillations by appropriate baffling and to observe the effect upon the clear liquid head results. It is believed that physically

meaningful corrections can be applied to the steady-state results to predict the hydraulic behavior in vented cyclic operation.

5. Sealed Steady-State and Cyclic Operation

Although no reliable quantitative studies have been made either at steady-state or in the controlled-cyclic mode with all column sections sealed, some qualitative observations are available. It has been noted that although the liquid holdups and interstage pressure differences on the lower trays were similar in magnitude, those on the top plate were always found to be much larger, sometimes by factors of three or four. In the cyclic mode, this problem became extremely serious, and holdups of as much as 6 inches of clear liquid have been observed on the top stage at liquid flow rates around 2 gallons per minute.

It is feared that many of the problems encountered are the result of liquid-flow end effects. At the top of the column the liquid phase is introduced onto the highest tray through a perforated-pipe distributor. The liquid streams leaving the distributor have velocities much higher than the drainage velocity from a tray insert, and this may result in a greater entrainment of air bubbles into the gas space below the top plate. It has already been mentioned that column operation may be sensitive to the amount of air entrained in the drain-line liquid. This is undesirable, since drain-line configurations may dif-

fer considerably from one unit to the next, yet it is desired to make the hydraulic performance as uniform as possible. A solution suggested by Gerster and Scull (6) was to vent the bottom section through a valve. Clearly, if the rate of air flow through the partly-opened valve is considerably larger than that through the drain line, the buildup of pressure is under the control of the operator and not at the mercy of spurious effects due to column drain configuration. In an actual column the vent line would probably be connected from the bottom section of the column to the top.

Considerations of good column design seem also to favor some sort of variable-venting scheme to increase the liquid residence-time on a tray. Calculations (Appendix VIII.C.5) show that for a completely-vented tray with 1/8-inch holes and 10% free area the mean liquid residence time is around 0.6 second. Liquid flow period lengths of this order are too small to be of much commercial interest, so it is desirable to find some means to increase the liquid holdup at a given liquid flow rate. This can be accomplished by reducing the fractional perforated area, but a reduction in free area will also increase the pressure drop of the gas during the VFP. One solution to this problem is to allow the pressure-difference in the gas phase to oppose the drainage of liquid through the holes; moreover, it may be

possible to control tray liquid holdups throughout the column by manipulation of the venting valve in the bottom section.

Another problem with vented cyclic operation is that to obtain a ratio of molal gas flow rate to molal liquid flow rate of order unity, the gas flow period must be twenty to fifty times as long as the liquid flow period. With such large τ_G/τ_L ratios, it is feared that weepage of liquid during the vapor flow period would become prohibitive. This problem would be made much less serious by partial venting to decrease the allowable LFP liquid rate.

B. Liquid Mixing.

Although no in-rig experiments on axial liquid mixing have been conducted, the probes, bridge circuits, and recorder have been tested by performing a simple stirred-tank residence-time study and observing the decay of solution conductivity with time. The value of mean residence-time determined from the recorded exponential curve was found to be in excellent agreement with that calculated from the known flowrate and tank volume.

Another experiment was conducted to assess the effect of noise due to bubbles in the liquid phase upon the measured voltage signal. It was found that severe high frequency fluctuations in voltage signal made measurements quite difficult, so that filtering of the response was considered necessary for accurate measurements. Accordingly, a filter box was constructed, containing two iden-

tical 2nd-order, low-pass, operational amplifier circuits designed to attenuate the noise frequencies by a factor of 100 with no appreciable influence upon the form of the measurement signals. It was found that this arrangement successfully eliminated bubble-noise, but that the time-average electrical conductivity of the aerated liquid was lower than that for clear liquid having the same salt concentration.

This dependence of solution conductivity upon degree of aeration of the liquid phase is unfortunate in that it necessitates careful calibration of the probes under the same hydraulic conditions to be used in a particular run. The voltage signals corresponding to the maximum and minimum salt concentrations in the aerated liquid must be known accurately in order to normalize the response signals properly. On the other hand, the measurement of departures from non-aerated behavior gives an estimate of voidage fractions which are difficult to measure accurately by comparing froth height with clear liquid height.

C. Mathematical Simulation Models:

1. Hydraulics.

In order to facilitate the correlation of data for liquid flow with an opposing gas-phase pressure difference and non-negligible surface tension effects a semi-empirical flow model has been developed. Previous investigators have suggested that the behavior of a particular perforation on a sieve plate is deter-

mined by the instantaneous net pressure difference across it, and that fluctuations in gas-phase pressures and liquid heads may result in bubbling of gas, draining of liquid, or bridging at any instant of time and any location. Prince and Chan (15) attempted to cast this quantitative picture into a very simple mathematical representation, which assumed that superimposed upon the mean pressure difference was a small fluctuating pressure having the value $+\Delta P_f$ at holes which were bubbling gas and $-\Delta P_f$ at holes which were draining liquid. The possibility of bridging with no flow of either phase was neglected. The fraction of holes bubbling was then selected to minimize the pressure-fluctuation, ΔP_f.

The principal shortcoming in this approach was that it failed to include any information on the physical processes causing the fluctuation. As a result, it is found that an additional equation must be supplied in order to predict gas and liquid flow rates from the mean pressure difference. Also, since bridging of holes is commonly observed in the case of trays with perforation-diameters of 1/4-inch or smaller, the neglect of this effect could introduce serious errors.

These difficulties can be overcome by substituting for the minimization-of-pressure-fluctuation condition, the physically realistic assumption that pressure-fluctuation amplitudes are random quantities

having some distribution of values about a zero mean. If the spread of the distribution is sufficiently large, it is possible to have finite probabilities for each of the three possible states. From momentum-balances for gas and liquid flow, one may deduce "expectation values" for the flowrates if the parameters of the distribution are known, or, for a given distribution shape, the parameters of the distribution may be deduced from data. The details of the model equations and their use are discussed in Appendix VIII.B.

Thus far it has been virtually impossible to use the model for data interpretation, not because of any inherent shortcoming in the mathematical representation, but because the data obtained from the single tray insert used have not been sufficiently conclusive to permit evaluation of all necessary input quantities. As mentioned in the discussion of hydraulic results, the actual discharge relationship has been obscured by surface-tension effects at the low-flowrate end and by air entrainment at all flowrates. For interpretation of the variable-venting results, the dependence of air entrainment rate upon both liquid flowrate and clear liquid head must be specified. For a single tray insert these two variables are strongly coupled and the individual dependences are practically impossible to determine unless the exact form of the desired correlation is known.

2. Mass-transfer Model with Mixing.

The complete mass-transfer simulation model of Gerster and Scull (6) has been programmed for use on an IBM 1130 computer. The program can handle short (less than 6 stages) columns with computation times on the order of 30 seconds; conversion for use on larger, faster machines, such as the IBM 371 system, is straightforward and will essentially remove all limitations on total core storage and solution time.

The dimensionless differential and algebraic equations are summarized in Appendix VIII.C., together with some typical simulation results. The differential equations are integrated numerically using a 4-th order Runge-Kutta algorithm, and stable cyclic solutions are obtained by simulating the startup of a column from an assumed set of initial conditions until the periodicity conditions are satisfied within a certain tolerance. Much of the programming and all of the simulation experiments were carried out by Miss D. Jarmoluk, a graduate assistant working on the project.

The program is prepared to generate results, once correlations for hydraulic variables and mixing parameters have been developed.

VI. Direction of Current and Future Work.

As suggested in the discussion of results, it is anticipated that repetitions of some of the experimental studies using trays of different free area fraction will provide the needed infor-

mation on the intrinsic head-vs.-liquid flowrate and air entrainment rate vs. liquid flow rate and head relations. Once such information is available, the flow model can be brought into play to assess the relative effects of liquid aeration and pressure fluctuations upon the liquid heads and pressures measured in partially-vented steady-state experiments.

Currently, a series of experiments is being conducted to measure the quantitative effects of changing flow-period lengths in vented cyclic operation. It is hoped that the weepage mechanism postulated to explain some of the observed departures from steady-state hydraulics can be made more quantitative, and that other contributing phenomena can be postulated and verified by examination of the data.

The electronic circuits developed for the salt-tracer mixing studies and the associated hardware for two-supply cyclic operation await their first in-rig test. It will probably be found desirable to adjust the rates of air venting from the various sections, in order to increase the liquid residence time to around 2 seconds for experimental convenience. It may be found that tracer experiments also give information on weepage rates and other hydraulic phenomena which will be useful in interpreting the previous hydraulic data.

Once a model for column operation is formulated, it should be tested by carrying out absorption experiments in a well-designed cyclic column as suggested in the section on long-term objectives. The results of such a study should be helpful in suggesting alternate design configurations and modes of operation.

VII. Summary.

Hydraulic experiments carried out in a 3-tray cyclic column, using air and water as the counterflowing phases, have indicated the form of the gas- and liquid-phase discharge relationships, the importance of air-bubble entrainment in the liquid phase, and the effect of flow-period lengths in producing departures from steady-state liquid heads in vented cyclic operation. Equipment for measurement of mixing parameters has been assembled and tested and computer programs and simulation models have been developed for interpretation of experimental data and prediction of cyclic column performance. It remains to complete the cyclic hydraulics and liquid mixing studies, and to use different tray inserts to finalize the steady-state hydraulic relationships.

VIII. Appendix

A. Models for Axial Liquid Mixing in Cyclic Operation.

1. Liquid-phase Mixing from Evolution of Vertical Concentration-Distance Profile.

If the mixing in the liquid phase (excluding the falling liquid streams) is assumed to be described by a "dispersion coefficient", then in analogy with Fick's law,

$$\frac{\partial c}{\partial \theta} + \frac{\partial c}{\partial \xi} = \frac{1}{Pe}\frac{\partial^2 c}{\partial \xi^2} \qquad \text{(A.1-1)}$$

in normalized coordinates. The boundary conditions suggested by Danckwerts apply:

$$\begin{aligned} &1. \quad c = 0 \quad \text{at} \quad \theta = 0, \ \text{for all } \xi. \\ &2. \quad 1 = c - \frac{1}{Pe}\frac{\partial c}{\partial \xi} \quad \text{at} \quad \xi = 0, \ \theta > 0. \\ &3. \quad \frac{\partial c}{\partial \xi} = 0 \quad \text{at} \quad \xi = 1, \ \theta > 0. \end{aligned} \qquad \text{(A.1-2)}$$

The infinite-series solution to this problem has the form,

$$c(\theta,\xi) = 1 - \sum_{n=1}^{\infty} A_n \exp\left\{-\frac{(1+\gamma_n^2)Pe}{4}\theta\right\} \cdot \exp\left\{\frac{\xi Pe}{2}\right\} \cdot \frac{1}{\sqrt{1+\gamma_n^2}} \sin\left\{\frac{\gamma_n Pe}{2}\xi + \phi_n\right\}, \qquad \text{(A.1-3)}$$

where,

$$A_n = \frac{-\left[\frac{4\gamma_n}{Pe(4+\gamma_n^2)}\right]}{\left[\frac{(1+\gamma_n^2)}{2} + \frac{2}{Pe}\right]}, \qquad \text{(A.1-4)}$$

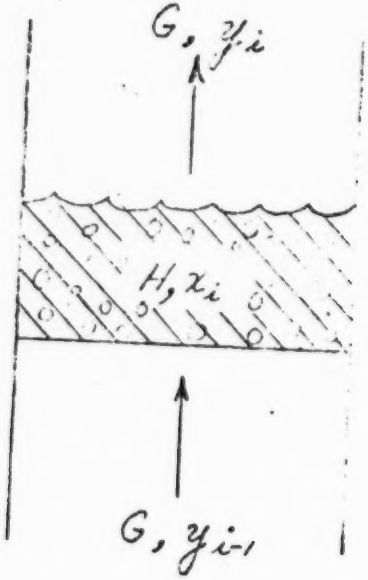

Equilibrium:

$$y_i^* = m x_i$$

VFP Variables

FIGURE 10

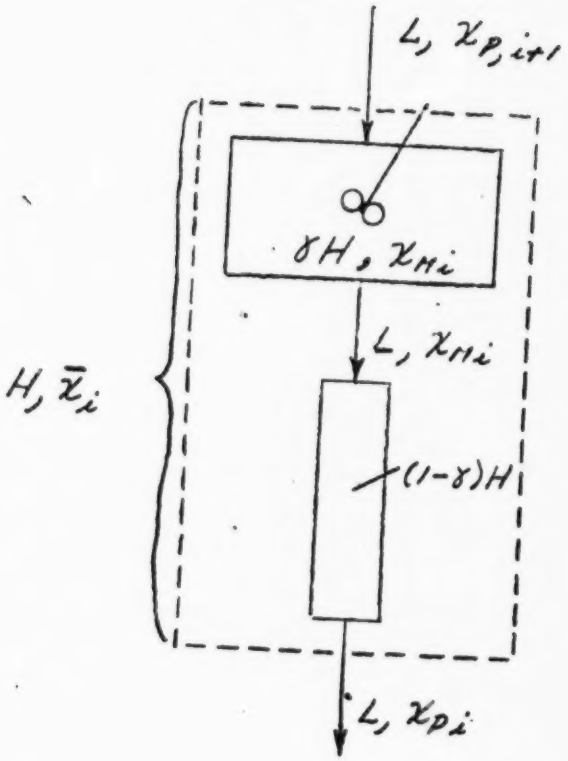

LFP Mixing-Model

FIGURE 11

y_n is the n-th eigenvalue solving,

$$\tan\left(\frac{y_n Pe}{2}\right) = \frac{2y_n}{y_n^2 - 1} , \qquad \text{(A.1-5)}$$

and $$\phi_n = \tan^{-1} y_n . \qquad \text{(A.1-6)}$$

The predicted functional form can be fitted, in a least-squares sense, to data on concentration vs. distance and time, by choice of the Peclet number, Pe.

2. Overall Mixing Parameter from Measurements of Well-Mixed VFP Liquid Composition.

Let, $$\left(\frac{\chi(\theta) - \chi(0)}{\chi_i - \chi(0)}\right) \equiv \bar{f}(\theta) . \qquad \text{(A.2-1)}$$

Then, for cycle #1,

$$\left(\frac{\chi_1(1) - \chi_{10}}{\chi_{1f} - \chi_{10}}\right) = \bar{f}(1) , \qquad \text{(A.2-2)}$$

and for cycle #2,

$$\left(\frac{\chi_2(1) - \chi_{20}}{\chi_{2f} - \chi_{20}}\right) = \bar{f}(1) . \qquad \text{(A.2-3)}$$

For periodicity,

$$\chi_1(1) = \chi_{20} \quad \text{and} \quad \chi_2(1) = \chi_{10} . \qquad \text{(A.2-4)}$$

so that, $$\chi_{10} = \frac{\chi_{2f} + (1 - \bar{f}(1))\chi_{1f}}{2 - \bar{f}(1)} , \qquad \text{(A.2-5)}$$

$$\chi_{20} = \frac{\chi_{1f} + (1 - \bar{f}(1))\chi_{2f}}{2 - \bar{f}(1)} . \qquad \text{(A.2-6)}$$

$$\therefore \quad \left(\frac{\chi_{10} - \chi_{20}}{\chi_{2f} - \chi_{1f}}\right) \equiv R = \frac{\bar{f}(1)}{2 - \bar{f}(1)} . \qquad \text{(A.2-7)}$$

Hence, $$\bar{f}(1) = \frac{2R}{1 + R} . \qquad \text{(A.2-8)}$$

The mixing-model equations are,

$$\frac{d\bar{f}_M}{d\theta} = \frac{\phi}{\gamma}(1-\bar{f}_M) \qquad \text{(A.2-9)}$$

$$\bar{f}_M(0) = 0$$

$$\frac{d\bar{f}}{d\theta} = \phi(1-\bar{f}_D)$$

$$\bar{f}(0) = 0 \qquad \text{(A.2-10)}$$

$$\bar{f}_D(\theta) = \begin{cases} 0 & , \text{ for } \theta \le \frac{1-\gamma}{\phi} \\ \bar{f}_M(\theta - \frac{1-\gamma}{\phi}) & , \text{ for } \theta > \frac{1-\gamma}{\phi} \end{cases} \qquad \text{(A.2-11)}$$

The solution is,

$$\bar{f}(1) = \begin{cases} \phi & , \text{ for } \frac{1-\gamma}{\phi} \ge 1 \\ 1-\gamma e^{-(1-\frac{1-\gamma}{\phi})} & , \text{ for } \frac{1-\gamma}{\phi} < 1 \end{cases} \qquad \text{(A.2-12)}$$

Hence,

$$\frac{2R}{1+R} = \begin{cases} \phi & , \text{ for } \frac{1-\gamma}{\phi} \ge 1 \\ 1-\gamma e^{-(1-\frac{1-\gamma}{\phi})} & , \text{ for } \frac{1-\gamma}{\phi} < 1 \end{cases} \qquad \text{(A.2-13)}$$

from which γ can be determined if $\phi > 1-\gamma$

The case $\phi \le 1-\gamma$ means that the mixing situation cannot be distinguished from plug flow.

B. Model for Gas and Liquid Flows Through a Perforated Plate.

It has been suggested that "simultaneous" flows of gas and liquid through a perforated plate at steady-state may result from pressure and liquid-head fluctuations which bias the holes positively or negatively. Thus, at any given hole any one of three possible conditions may exist at any given time:

1. Bubbling of gas up through the hole.
2. Draining of liquid down through the hole.
3. Bridging, with no flow of either phase.

If we may assume for simplicity that the pressure drop of a continuous medium flowing through a perforation is a constant multiple of the velocity-head based on the cross-sectional area of the hole, the following approximate steady-state momentum balances may be written:

1. For the gas phase,

$$C_G \frac{\rho_G u_G^2}{2 g_c} = \Delta P_G - \rho_L h - \Delta P_S + \Delta P_f , \qquad \text{(B-1)}$$

$$\text{when} , \quad (\Delta P_G - \rho_L h) + \Delta P_f > \Delta P_S .$$

2. For the liquid phase,

$$C_L \frac{\rho_L u_L^2}{2 g_c} = -\Delta P_G + \rho_L h - \Delta P_S - \Delta P_f + \rho_L T_P , \qquad \text{(B-2)}$$

$$\text{when} , \quad (\Delta P_G - \rho_L h) - \rho_L T_P + \Delta P_f < -\Delta P_S .$$

3. For bridging,

$$-\Delta P_S + \rho_L T_P \leq (\Delta P_G - \rho_L h) + \Delta P_f \leq \Delta P_S . \qquad \text{(B-3)}$$

The basic assumption upon which the flow model rests can be stated as follows:

The pressure-fluctuation, ΔP_f, is a random variable, in the probabalistic sense, whose density function, $p(\Delta P_f; \sigma)$ will be assumed to have the following properties:

1. A mean of zero.
2. An index of deviation from the mean, σ.
3. Symmetry about the mean; i.e.,

$$p(\Delta P_f; \sigma) = p(-\Delta P_f; \sigma).$$

Before proceeding to derive the relationships for average gas and liquid flowrates, it is advantageous to cast the preceeding momentum balances into a more symmetrical form. Thus,

$$C_G \frac{\rho_G u_G^2}{2g_c} = (\Delta P_G - \rho_L h - \tfrac{1}{2}\rho_L T_P) - (\Delta P_S - \tfrac{1}{2}\rho_L T_P) + \Delta P_f, \tag{B-4}$$

$$C_L \frac{\rho_L u_L^2}{2g_c} = -(\Delta P_G - \rho_L h - \tfrac{1}{2}\rho_L T_P) - (\Delta P_S - \tfrac{1}{2}\rho_L T_P) - \Delta P_f. \tag{B-5}$$

Now, define,

$$\delta = (\Delta P_G - \rho_L h - \tfrac{1}{2}\rho_L T_P) + \Delta P_f, \tag{B-6}$$

$$\delta_o = (\Delta P_G - \rho_L h - \tfrac{1}{2}\rho_L T_P), \tag{B-7}$$

and

$$\gamma = (\Delta P_S - \tfrac{1}{2}\rho_L T_P). \tag{B-8}$$

Clearly, then,

1. For gas bubbling, $\delta > \gamma$,
2. For liquid draining, $\delta < -\gamma$,
3. For bridging, $-\gamma \leq \delta \leq \gamma$,

and,

$$u_G = \left(\frac{2g_c}{C_G \rho_G}\right)^{1/2} \sqrt{\delta - \gamma}, \quad \delta > \gamma, \tag{B-9}$$

$$u_L = \left(\frac{2g_c}{C_L \rho_L}\right)^{1/2} \sqrt{-\delta - \gamma}, \quad \delta < -\gamma. \tag{B-10}$$

From the basic assumption it is easily shown that the density function for the "net pressure difference," δ, has a mean of δ_o, an index of deviation of σ, and symmetry about the new mean. It may be represented as

$$p(\delta-\delta_o;\sigma) .$$

The probability of each of the three types of flow behavior may now be calculated.

1. Probability of gas bubbling $= \beta_1$

$$= \int_{\gamma}^{\infty} p(\delta-\delta_o;\sigma)\,d\delta ; \qquad \text{(B-11)}$$

2. Probability of liquid draining $= \beta_2$

$$= \int_{-\infty}^{-\gamma} p(\delta-\delta_o;\sigma)\,d\delta ; \qquad \text{(B-12)}$$

3. Probability of bridging $= \beta_3$ (B-13)

$$= \int_{-\gamma}^{\gamma} p(\delta-\delta_o;\sigma)\,d\delta .$$

It can be shown that the expectation values of average gas and liquid velocities (based on total perforated area) are,

$$\langle u_G\rangle = \left(\frac{2g_c}{C_G\rho_G}\right)^{1/2}\int_{\gamma}^{\infty}(\delta-\gamma)^{1/2}p(\delta-\delta_o;\sigma)\,d\delta ; \qquad \text{(B-14)}$$

and, $$\langle u_L\rangle = \left(\frac{2g_c}{C_L\rho_L}\right)^{1/2}\int_{-\infty}^{-\gamma}(-\delta-\gamma)^{1/2}p(\delta-\delta_o;\sigma)\,d\delta . \qquad \text{(B-15)}$$

If all pressure-differences and velocities are made dimensionless by the transformations,

$$\lambda = \delta/\sigma \;;\; \lambda_o = \delta_o/\sigma \;;\; \beta = \gamma/\sigma ;$$

$$\langle u_G\rangle^* = \langle u_G\rangle \Big/ \left(\frac{2g_c\sigma}{C_G\rho_G}\right)^{1/2} ; \qquad \text{(B-16)}$$

$$\langle u_L\rangle^* = \langle u_L\rangle \Big/ \left(\frac{2g_c\sigma}{C_L\rho_L}\right)^{1/2} .$$

then, $$\langle u_G\rangle^* = \int_{\beta}^{\infty}(\lambda-\beta)^{1/2}p(\lambda-\lambda_o;1)\,d\lambda ; \qquad \text{(B-17)}$$

and, $$\langle u_L\rangle^* = \int_{-\infty}^{-\beta}(-\lambda-\beta)^{1/2}p(\lambda-\lambda_o;1)\,d\lambda . \qquad \text{(B-18)}$$

Now, introduce the new variables,

$$z = \lambda - \lambda_o \ , \qquad y = \lim_{z \to \xi - \lambda_o} z = \xi - \lambda_o \ . \tag{B-19}$$

Then,

$$\langle u_G \rangle^* = \int_y^\infty (z-y)^{1/2} p(z;1)\, dz \ .$$

for gas flow. For liquid flow, let

$$z = -\lambda - \lambda_o \ , \qquad y = -\xi - \lambda_o \ , \tag{B-21}$$

whence it can be shown that

$$\langle u_L \rangle^* = \int_y^\infty (z-y)^{1/2} p(z;1)\, dz \ . \tag{B-22}$$

If we let,

$$f(y) \equiv \int_y^\infty (z-y)^{1/2} p(z;1)\, dz \ , \tag{B-23}$$

then,

$$\langle u_G \rangle^* = f(\xi - \lambda_o) \ , \tag{B-24}$$

and,

$$\langle u_L \rangle^* = f(-\xi - \lambda_o) \ . \tag{B-25}$$

One point of hydraulic data consists of experimental values for the quantities,

$$\{ \langle u_G \rangle, \langle u_L \rangle, \delta_o \} \ .$$

Since we have two relations to determine σ, the "spread" of the pressure fluctuation, we may select a σ which minimizes the sum of squares of errors for the two constraints.

Since δ_o is a difficult quantity to measure experimentally, however, the recommended procedure is to solve the two equations exactly for σ and δ_o, knowing $\langle u_G \rangle$ and $\langle u_L \rangle$. The agreement of measured and calculated δ_o-values constitutes a test of the predictive power of the model (using the chosen density-function) while σ is a single empirical parameter which can be correlated.

The "flowrate correlation" is completely specified by,

1. A probability density function, p.
2. An empirical correlation for σ, the deviation from the mean pressure-difference.

C. Mathematical Model for Mass-Transfer and Liquid Mixing in a Cyclic Absorber.

The mathematical model equations originally suggested by McWhirter and Lloyd (14) and modified by Gerster and Scull (6) to account for the effects of axial liquid mixing are summarized for a general stage as follows:

1. Gas Flow Period.

Assuming constant and equal liquid holdups, H, and equal Murphree point efficiencies, η, on all stages; a constant molal gas flowrate, G'; and a dilute gas phase with Henry's law constant, m; an unsteady state component material balance on the i-th stage (see Figure 10) gives,

$$\frac{dx_i}{dt} = \frac{G'}{H}(y_{i-1} - y_i) \qquad \text{(C-1)}$$

$$x_i(0) = x_{i0}$$

The composition of the gas stream leaving the stage is related to the composition of the gas stream entering the stage and to the tray liquid composition by the Murphree efficiency,

$$\eta = \frac{y_i - y_{i-1}}{m x_i - y_{i-1}} \quad . \tag{C-2}$$

2. Plug-Flow Conditions.

If during the liquid flow period a fraction ϕ of a tray holdup is dropped down the column without mixing, the resulting composition on the i-th tray at the end of the liquid flow period is,

$$\bar{x}_i(\tau_i) = \begin{cases} x_T \quad , \text{ if } i \geq n-k+1 \, , \\ (l-\phi)\, x_{i+k}(\tau_G) + (\phi - k)\, x_{i+l}(\tau_G) \, , \\ \qquad \text{if } i < n-k+1 \, , \end{cases} \tag{C-3}$$

where, k and l are consecutive integers such that

$$k \leq \phi < l \quad , \quad \text{and} \quad x_{n+1}(\tau_G) = x_T \, .$$

3. Mixing-Model Equations.

To generalize the mixing of liquid we assume, as an alternative to the plug-flow conditions, a mixing model in which the fraction, γ, of the liquid holdup is assumed to be well-stirred, while the remaining fraction, $(1-\gamma)$, is in plug flow. (See Figure 11). Then a material balance on the stirred cell gives,

$$\frac{dx_{M,i}}{dt} = \frac{\phi}{\gamma \tau_L} (x_{D,i+1} - x_{M,i}) \tag{C-4}$$

$$x_{M,i}(0) = x_i(\tau_G) \, .$$

and an overall balance on the entire tray holdup gives for the average tray liquid composition,

$$\frac{d\bar{x}_i}{dt} = \frac{\phi}{\tau_L}(x_{p,i+1} - x_{p,i})$$
$$\bar{x}_i(0) = x_i(\tau_G). \qquad \text{(C-5)}$$

The composition of liquid leaving the plug-flow section at any time is,

$$x_{p,i}(t) = \begin{cases} x_i(\tau_G) & , \text{ for } t \le t_R \\ x_{H,i}(t - t_R) & , \text{ for } t > t_R , \end{cases}$$

where
$$t_R = \frac{(1-\delta)\tau_L}{\phi} . \qquad \text{(C-6)}$$

4. Periodicity Conditions.

Compositions at the end of the LFP are related to initial VFP compositions by,

$$x_{i0} = \bar{x}_i(\tau_L) . \qquad \text{(C-7)}$$

5. Average Exit-Gas Composition.

In order to calculate the number of theoretical stages to accomplish the given separation, it is necessary to compute the average exit-gas composition.

For the plug-flow case, an overall solute material balance for all flows during one cycle gives,

$$\bar{y}_{OUT} = y_B - \frac{\phi H}{G'\tau_G}\left(\frac{1}{\phi} f(\phi) - x_T\right), \qquad \text{(C-8)}$$

with,

$$f(\phi) = \begin{cases} \phi\, x_i(\tau_G) , & \text{for } \phi \le 1 \\ \sum_{i=1}^{k} x_i(\tau_G) + x_{k+1}(\tau_G)\cdot(\phi - k) , & \text{for } \phi > 1 , \end{cases} \qquad \text{(C-9)}$$

and k and 1 are previously-defined integers.

For the generalized mixing model case,

$$\bar{y}_{OUT} = y_B - \frac{\phi H}{G' \tau_G} \left(\bar{x}_B(\tau_L) - x_T \right), \quad \text{(C-10)}$$

where, $\bar{x}_B(\tau_L)$ is defined by,

$$\frac{d\bar{x}_B}{dt} = \frac{1}{\tau_L} x_{P,1}$$
$$\bar{x}_B(0) = 0. \quad \text{(C-11)}$$

6. Overall Column Efficiency.

Colburn's analytical solution for the number of theoretical plates required to accomplish a given separation is, (C-12)

$$N_C = \begin{cases} \left(\frac{y_B - m x_T}{\bar{y}_{OUT} - m x_T} \right) - 1 & , \text{ for } A = 1 \\ \frac{\ln \left\{ \left(\frac{y_B - m x_T}{\bar{y}_{OUT} - m x_T} \right) \left(1 - \frac{1}{A} \right) + \frac{1}{A} \right\}}{\ln (A)} & , \text{ for } A \neq 1, \end{cases}$$

$$A = \frac{L}{mG} = \frac{\phi H}{m G' \tau_G} . \quad \text{(C-13)}$$

The overall efficiency of the cyclic column is, then,

$$E_o = N_C / N \times 100\% . \quad \text{(C-14)}$$

7. Dimensionless Form.

The foregoing equations may be cast into dimensionless form by means of the following transformations:

$$\xi_i = \frac{x_i - x_T}{y_B/m - x_T} \quad ; \quad \xi_i' = \frac{y_i/m - x_T}{y_B/m - x_T}$$

$$\theta = \begin{cases} t/\tau_L \text{ , in LFP} \\ t/\tau_G \text{ , in VFP} \end{cases} \quad ; \quad A = \frac{\phi H}{m G' \tau_G} .$$

(C-15)

For gas flow:

$$\frac{d\bar{f}^{e}_{i}}{d\theta} = \frac{\phi}{A}\left(f^{e}_{i-1}{}' - f^{e}_{i}{}'\right),$$

$$f^{e}_{i}(0) = \bar{f}^{e}_{i}(1)$$

$$\eta = \frac{f^{e}_{i}{}' - f^{e}_{i-1}{}'}{f^{e}_{i} - f^{e}_{i-1}}, \qquad \text{(C-16)}$$

$$f^{e}_{B}{}' = 1.$$

For plug flow:

$$\bar{f}^{e}_{i}(1) = \begin{cases} f^{e}_{T} = 0 \quad , \text{ for } i \geq n-k+1 \\ (l-\phi) f^{e}_{i+k}(1) + (\phi - k) f^{e}_{i+l}(1), \\ \qquad \text{for } i < n-k+1 . \end{cases}$$

(C-17)

For generalized mixing:

$$\frac{d f^{e}_{M,i}}{d\theta} = \frac{\phi}{\gamma}\left(f^{e}_{P,i+1} - f^{e}_{M,i}\right),$$

$$f^{e}_{M,i}(0) = f^{e}_{i}(1)$$

$$\frac{d\bar{f}^{e}_{i}}{d\theta} = \phi\left(f^{e}_{P,i+1} - f^{e}_{P,i}\right),$$

$$\bar{f}^{e}_{i}(0) = f^{e}_{i}(1)$$

$$f^{e}_{P,i}(\theta) = \begin{cases} f^{e}_{i}(1), & 0 \leq \theta \leq \frac{1-\gamma}{\phi} \\ f^{e}_{M,i}\left(\theta - \frac{1-\gamma}{\phi}\right), & \theta > \frac{1-\gamma}{\phi} \end{cases},$$

$$f^{e}_{T} = 0. \qquad \text{(C-18)}$$

For average exit gas composition:

in plug flow,

$$\bar{f}'_{OUT} = 1 - A f'(\phi) ,$$

where,

$$f'(\phi) = \begin{cases} f_{,(1)} & , \text{ for } \phi \leq 1 \\ \sum_{i=1}^{k} \phi f_{i(1)} + f_{k(1)} \cdot \left(\frac{\phi - k}{\phi}\right) , & \text{for } \phi > 1. \end{cases}$$

or, for generalized mixing, (C-19)

$$\bar{f}'_{OUT} = 1 - A \bar{f}_B(1) ,$$

where $$\frac{d\bar{f}_B}{d\theta} = f_{B,1} , \quad \text{(C-20)}$$

with $$\bar{f}_B(0) = 0.$$

For overall column efficiency:

$$N_C = \begin{cases} 1/\bar{f}'_{OUT} - 1 & , \quad A = 1 \\ \dfrac{\ln\left\{1/\bar{f}'_{OUT}\left(1 - \frac{1}{A}\right) + \frac{1}{A}\right\}}{\ln(A)} & , \quad A \neq 1 \end{cases} \quad \text{(C-21)}$$

and $$E_o = N_C/N \times 100\% . \quad \text{(C-22)}$$

The overall column efficiency,

$$E_o = E_o(N, \phi, A, \eta, \gamma) ,$$

is a function of 5 dimensionless parameters. It has become customary to illustrate this relationship for plug-flow by plotting E_o as a function of ϕ, yielding a curve with cusp-like maxima at the first N positive integral values of ϕ. Such a plot is shown in Figure 12, for $\gamma = 0$. For values of the mixing parameter $\gamma > 0$, the solution curves break off

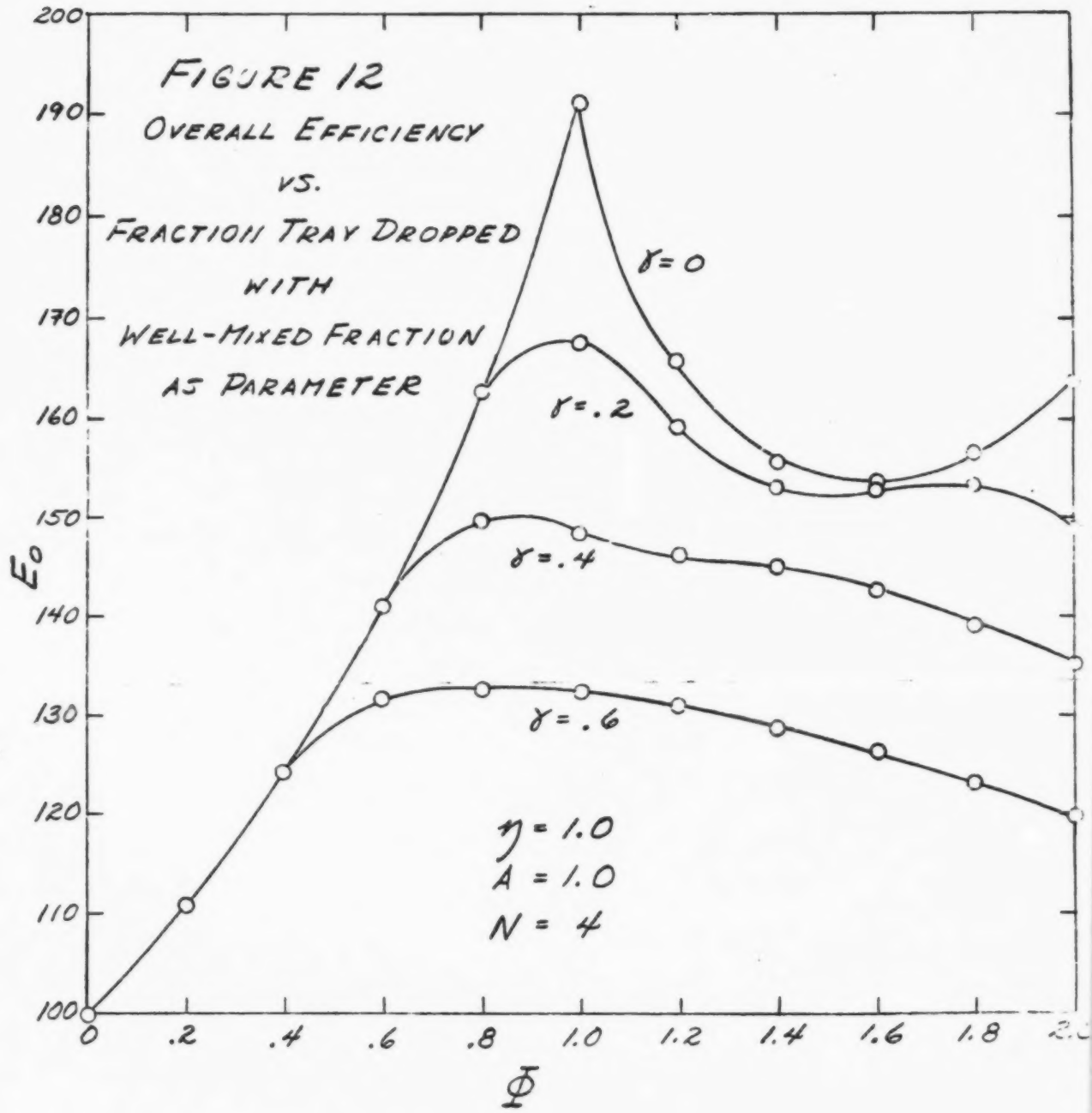
FIGURE 12
OVERALL EFFICIENCY
VS.
FRACTION TRAY DROPPED
WITH
WELL-MIXED FRACTION
AS PARAMETER
γ = 0
γ = .2
γ = .4
γ = .6
η = 1.0
A = 1.0
N = 4
E0
Φ
200
190
180
170
160
150
140
130
120
110
100
0
.2
.4
.6
.8
1.0
1.2
1.4
1.6
1.8

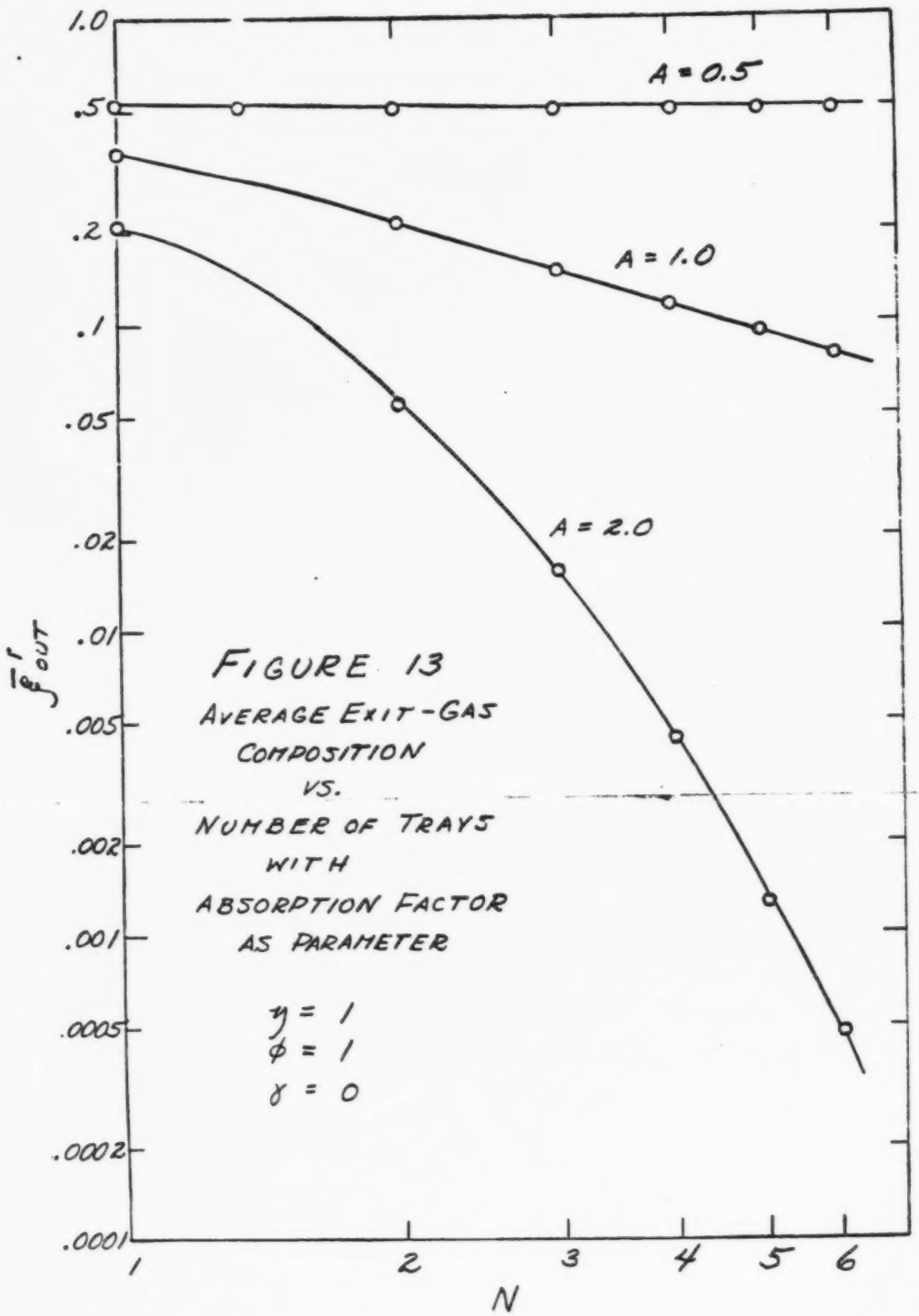

FIGURE 13

AVERAGE EXIT-GAS COMPOSITION VS. NUMBER OF TRAYS WITH ABSORPTION FACTOR AS PARAMETER

$\eta = 1$
$\phi = 1$
$\gamma = 0$

from the plug-flow solution at $\phi = (1-\gamma)$ and show flatter and less well-defined maxima at lower values of overall efficiency.

Colburn's equation is normally plotted as log normalized exit-gas composition vs. log(1+ number of theoretical trays), with absorption factor as a parameter. A similar plot for the cyclic case illustrates the improvement in separation. (Figure 13.)

D. Sample Calculations.

1. Comparison of Experimental Slope of Liquid-Head vs. Flow Rate with Hagen-Poiseuille Law:

$$Q = \frac{\pi g \rho_L \Delta H D^4}{128 \mu L} \quad , \qquad \text{(D.1-1)}$$

D = 1/8 inch = 1/96 ft.

L = 1/4 inch = 1/48 ft.

$\Delta H = \Delta h$(inches)/12 ft.

ρ_L = 62.4 lbs/ft.^{2}

g = 32.2 ft/sec^2

μ = 6.72 x 10^{-4} lb/(ft.sec)

Q = q (gallons/min.) x 2.228 x 10^{-3} ft^3/sec.

Therefore,

$$\Delta h (\text{in } H_2O) = \frac{(128)(6.72 \times 10^{-4})(12)(2.228 \times 10^{-3})(96)^4}{(48)(\pi)(32.2)(62.4)(230)} q(gp$$

$$\therefore \Delta h (\text{in. } H_2O) = 0.0028\, q\,(gpm).$$

Experimental value of slope = $\frac{0.4}{7.7} \frac{\text{inch}}{gpm} = .0519 \frac{\text{in. } H_2O}{gpm}$

2. Calculation of Flowrate for Critical Weber Number.

$$We_{crit} = \frac{\rho_L u_{crit}^2 D}{g \sigma} \qquad \text{(D.2-1)}$$

Thus, $$u_{crit} = \sqrt{\frac{We_{crit} g \sigma}{\rho_L D}}$$

Now, $$Q_{crit} = u_{crit} A = u_{crit} N \frac{\pi}{4} D^2$$

$$\therefore Q_{crit} = N \frac{\pi}{4} D^2 \sqrt{\frac{We_{crit} g \sigma}{\rho_L D}}$$

N = 230 holes

D = 1/96 ft.

g = 32.2 ft/sec^2

σ = .00495 lb/ft.

ρ_L = 62.4 lb/ft^3

So that, $$Q_{crit} = \frac{(230)(\pi)}{(4)(96)^2} \sqrt{\frac{(32.2)(.00495)(96)}{(62.4)}}\, We_{crit}^{1/2}$$

$$= .00971\ We_{crit}^{1/2} \quad ft.^3/sec.$$

$$\therefore q_{crit} = 4.356\ We_{crit}^{1/2} \quad gal./min.$$

The reported value of We_{crit} = 6.8 ; hence,

$$q_{crit} = 11.3 \text{ gpm}.$$

3. Effect of Liquid Aeration on Velocity-Head.

Basis: Equal volume flowrates of clear liquid.

If fractional aeration $\equiv \epsilon = \frac{q_{Air}}{q_{Air} + q_{H_2O}}$ (D.3-1)

$$\therefore \frac{\text{Volume of clear liquid}}{\text{Volume of aerated liquid}} = 1 - \epsilon \ . \qquad \text{(D.3-2)}$$

Density of aerated liquid ($\rho_{Gas} \sim 0$) is,

$$\rho_A = (1-\epsilon)\rho_L \ . \qquad \text{(D.3-3)}$$

Velocity of aerated liquid is,

$$u_A = \frac{u_L}{(1-\epsilon)} \ . \qquad \text{(D.3-4)}$$

$$\therefore \rho_A u_A^2 = \frac{1}{(1-\epsilon)} \rho_L u_L^2 \qquad \text{(D.3-5)}$$

For $\epsilon \doteq 0.25$,

$$\frac{\rho_A u_A^2}{\rho_L u_L^2} \doteq \frac{1}{.75} = 1.33,$$

or, a 33% increase in pressure drop over that for clear liquid.

4. Initial Rate of Pressure Rise Due to Air Flow Into a Sealed Column Section.

Assuming isothermal pressure increase,

$$PV_o = nRT_o , \qquad \text{(D.4-1)}$$

$$\therefore \left(\frac{dP}{dt}\right)_{t=0} = \left(\frac{RT_o}{V_o}\right)\left(\frac{dn}{dt}\right)_{t=0} . \qquad \text{(D.4-2)}$$

If the gas enters at the same conditions,

$$\left(\frac{dn}{dt}\right)_{t=0} = \left(\frac{P_o \dot{v}_{in}}{RT_o}\right) \qquad \text{(D.4-3)}$$

$$\text{So, } \left(\frac{dP}{dt}\right)_{t=0} = P_o \left(\frac{\dot{v}_{in}}{V_o}\right) . \qquad \text{(D.4-4)}$$

For a given small ΔP,

$$\Delta t = \left(\frac{\Delta P}{P_o}\right)\left(\frac{V_o}{\dot{v}_{in}}\right) .$$

P_o = 1 atm. = 407.0 inches of H_2O
ΔP = 1 inch of H_2O
V_o = 5500 cm^3
v_{in} = 200 cm^3/sec.

$$\therefore \Delta t = \left(\frac{1}{407}\right)\left(\frac{5500}{200}\right) = 0.068 \text{ sec.}$$

Initial pressure increase is 1 inch of H_2O in .068 sec.

5. Estimate of Liquid Residence-Time and Ratio of

Flow-Period Lengths.

a. The residence-time of liquid on a tray may be estimated from the measured values of liquid flow rate and clear liquid height as follows:

$$\text{Volume Holdup} \doteq \Delta H \cdot A_{Tray} \quad . \tag{D.5-1}$$

$$\therefore \quad \tau_R \doteq \frac{\Delta H \cdot A_{Tray}}{Q_{liq}} \quad . \tag{D.5-2}$$

Test case: ΔH = 1 inch H_2O = 1/12 ft H_2O
Q_{liq} = 13 gpm = .0290 ft^3/sec.
A_{Tray} = 0.196 ft^2

$$\therefore \quad \tau_R \doteq \frac{(0.196)}{(12)(.0290)} = 0.56 \text{ sec.}$$

b. To estimate the order of magnitude of the τ_G/τ_L ratio for vented cyclic operation, we make the following assumptions:

(1) Dry-plate pressure drop ~ clear liquid head ~ liquid velocity head.

$$\therefore \quad \rho_G u_G^2 \sim \rho_L u_L^2 \quad . \tag{D.5-3}$$

(2) Ratio of average molal gas and liquid flowrates of unity.

$$\therefore \quad \frac{\rho_G u_G \tau_G}{M_G} \sim \frac{\rho_L u_L \tau_L}{M_L} \quad . \tag{D.5-4}$$

From which,

$$\frac{\tau_G}{\tau_L} \sim \frac{M_G}{M_L}\left(\frac{\rho_L u_L}{\rho_G u_G}\right) \tag{D.5-5}$$

But,

$$\frac{\rho_L u_L}{\rho_G u_G} \sim \frac{u_G}{u_L} \sim \sqrt{\frac{\rho_L}{\rho_G}} \tag{D.5-6}$$

$$\therefore \quad \frac{\tau_G}{\tau_L} \sim \frac{M_G}{M_L}\sqrt{\frac{\rho_L}{\rho_G}} \quad . \tag{D.5-7}$$

With
M_G = 29 lb/lb-mole
M_L = 18 lb/lb-mole
P_L = 62.4 lb/ft^3
P_G = .075 lb/ft^3

$$\therefore \quad \frac{\tau_G}{\tau_L} \sim \frac{29}{18}\sqrt{\frac{62.4}{.075}} = 46.5 \, .$$

E. Nomenclature:

1. Appendix: A.1.

A_n = n-th coefficient term of series expansion, Eqn. (A.1-3)

C = tracer concentration normalized on [0,1].

n = subscript for terms in infinite-series solution

Pe = Peclet number

γ_n = n-th eigenvalue, solution of Eqn. (.1-5)

ϕ_n = phase angle for n-th eigenvalue, defined by Eqn. (A.1-6)

θ = dimensionsless time variable

ξ = dimensionless length variable

2. Appendix:

R = reduced concentration ratio, defined by Eqn. (A.2-7)

χ = average tracer concentration at any time

χ_{1f} = tracer concentration in LFP#1 feed.

χ_{2f} = tracer concentration in LFP#2 feed.

χ_{10} = tracer concentration at start of LFP#1

χ_{20} = tracer concentration at start of LFP#2

γ = well-mixed fraction

ϕ = fractional tray holdup dropped per cycle

θ = dimensionless time

$\bar{\xi}$ = reduced average tracer concentration

ξ_H = reduced tracer concentration in well-mixed cell.

ξ_P = reduced tracer concentration in stream leaving plug-flow section.

3. Appendix: B.

C_G = gas-phase discharge-loss coefficient

C_L = liquid-phase discharge-loss coefficient

h = clear liquid head on tray

ΔP_f = randomly-distributed pressure-fluctuation

ΔP_G = gas-phase pressure difference across tray

ΔP_S = pressure difference due to surface-tension required to form a drop or bubble.

T_p = tray thickness

U_G = instantaneous gas velocity through hole

U_L = instantaneous liquid velocity through hole

$\langle u_G \rangle$ = average gas velocity through holes

$\langle u_L \rangle$ = average liquid velocity through holes

$\langle u_G \rangle^*$ = reduced average gas velocity

$\langle u_L \rangle^*$ = reduced average liquid velocity

ζ = dimensionless dummy integration variable, defined by Eq'n (B-19) and Eq'n (B-21)

β_1 = probability that a hole will bubble gas

β_2 = probability that a hole will drain liquid

β_3 = probability that a hole will bridge

γ = modified surface-tension term, defined by Eq'n (B-8).

δ = modified randomly-distributed net pressure difference defined by Eq'n. (B-6).

δ_o = modified average net pressure-difference, defined by eq'n (B-7)

λ = reduced net randomly-distributed pressure-difference

λ_o = reduced average net pressure difference

ρ_G = gas density

ρ_L = liquid density

σ = index of deviation of random fluctuating pressure from the mean

η = integration limit defined by Eq'n (B-19) and Eq'n (B-21)

$\mathcal{F}$ = reduced surface-tension term

4. Appendix: C.

A = absorption factor defined by Eq'n (C-)

E_o = overall column efficiency

G = average molal gas flowrate for entire cycle

G' = actual molal gas flowrate during the VFP

H = molal tray liquid holdup

k = lower-bounding integer for

l = upper-bounding integer for

L = average molal liquid flow rate for entire cycle

m = Henry's law constant in mole-fraction units

N = number of stages in cyclic colujn

N_c = number of theoretical stages in a conventional column for same separation.

t = time variable

t_R = residence-time in plug-flow section

$\bar{x}_B$ = average bottom liquid composition variable

$\bar{x}_i$ = average tray composition in LFP on stage i

x_i = tray liquid composition in VFP on stage i

x_{io} = initial VFP liquid composition on stage i

$x_{m,i}$ = composition of well-stirred cell in LFP on stage i

$x_{p,i}$ = composition of liquid stream from plug-flow section in LFP on stage i

x_r = entering liquid composition

y_B = gas composition in entering stream

y_i = gas composition in stream leaving stage i

$\bar{y}_{avr}$ = average exit-gas composition variable

γ = fraction of tray holdup assumed well-mixed in LFP

ϕ = fraction of a tray holdup dropped per cycle

τ_C =VFP length

τ_L = LFP length

θ = reduced time variable

$\bar{\xi}_B$ = reduced bottom liquid-composition variable

ξ_i = reduced VFP tray liquid composition on stage i

$\bar{\xi}_i$ = reduced LFP average liquid composition on stage i

$\xi_{m,i}$ = reduced LFP well-mixed liquid composition on stage i

$\xi_{p,i}$ = reduced composition on liquid from plug-flow section during LFP on stage i

ξ_T = reduced entering liquid composition

ξ'_B = reduced gas composition in entering stream

ξ'_i = reduced gas composition in stream leaving stage i

$\bar{\xi}'_{OUT}$ = reduced average exit-gas composition variable.

η = Murphree point vapor efficiency

5. Appendix: D.1.

D = hole diameter

g = gravitational acceleration

Δh = clear liquid head, in. of H_2O

ΔH = clear liquid head, ft. of H_2O

L = length of short tube

q = liquid flowrate per hole, gallons/min

Q = liquid flowrate per hole, ft^3/sec

ρ_L = liquid density

μ = liquid viscosity

6. Appendix: D.2.

D = hole diameter

g = gravitational acceleration

N = number of perforations

q_{crit} = critical liquid rate for drop to jet transition, gallons/min.

Q_{crit} = critical liquid rate, $ft^3/sec.$

u_{crit} = critical liquid velocity

Nc_{crit} = critical Weber number

ρ_L = liquid density

σ = air-water surface tension

7. Appendix: D.3.

q_{Air} = flowrate of air through perforations by entrainment in the liquid phase.

q_{H_2O} = liquid flow rate

u_A = velocity of aerated liquid through holes

u_L = velocity of clear liquid through holes

ϵ = volume fraction of gas in gas-liquid mixture

ρ_A = density of aerated liquid

ρ_{Gas} = density of gas phase

ρ_L = density of clear liquid

8. Appendix: D.4.

n = number of moles of gas in closed volume

P = absolute pressure of gas in closed volume

P_o = initial absolute gas pressure

ΔP = small pressure increment

R = ideal-gas law constant

t = time-variable

Δt = small time-increment

$\dot{v}_{in}$ = rate of gas inflow

V_o = volume of gas space

9. Appendix: D.5.

A_{Tray} = column cross-sectional area

ΔH = clear liquid head

M_G = molecular weight of gas

M_L = molecular weight of liquid

Q_{liq} = liquid flow rate

U_G = gas velocity through holes

U_L = liquid velocity through holes

ρ_G = density of gas

ρ_L = density of liquid

τ_G = gas flow period length

τ_L = liquid flow period length

τ_R = approximate mean liquid residence time

10. Special Abbreviations:

VFP - vapor (gas) flow period

LFP - liquid flow period.

F. Literature Cited.

(1) Cannon, M. R., "A New Type of Distillation, Absorption and Extraction Column," Oil Gas J., 51, 268 (1952).

(2) Cannon, M. R., "Here's a New Liquid Extractor," Oil Gas J., 54 (Jan. 23), 68 (1956).

(3) Chien, H. H., J. T. Sommerfeld, V. N. Schrodt, and P. E. Parisot, "Study of Controlled Cyclic Distillation: II. Analytical Transient Solutions and Asymptotic Plate Efficiencies," Separation Science, 1, 281 (1966)

(4) Garcia, A., and A. R. Bayne, "Gas Flow Through Submerged Orifices," S. B. Thesis, Massachusetts Institute of Technology, 1965.

(5) Gaska, R. A., and M. R. Cannon, "Controlled Cycling Distillation in Sieve and Screen Plate Towers," Ind. Eng. Chem., 53, 630 (1961).

(6) Gerster, J. A., and H. M. Scull, "Performance of Tray Columns Operated in the Cycling Mode," AIChE J., 16, 108 (1970).

(7) Holland, C. D., "Multicomponent Distillation," Englewood Cliffs, N. J.: Prentice-Hall, Inc., 1963.

(8) Horn, F. J. M., "Periodic Countercurrent Processes," Ind. Eng. Chem., Process Design Develop., 6, 30 (1967).

(9) Lewis, W. K., Jr., "Rectification of Binary Mixtures," Ind. Eng. Chem., 28, 399 (1936).

(10) Lin, R. C., "Periodic Processes in Chemical Engineering," Ph.D. Thesis, Rice University, 1966.

(11) McAllister, R. A., P. H. McGinnis, and C. A. Plank, "Perforated-Plate Performance," Chem. Eng. Sci., 9, 25 (1958).

(12) McKay, D. L., and H. W. Goard, "Crystal Purification by Cyclic Solids Movement," Ind. Eng. Chem., Process Design Develop., 6, 16 (1967).

(13) McWhirter, J. R., and M. R. Cannon, "Controlled Cycling Distillation in a Packed-Plate Column," Ind. Eng. Chem., 53, 632 (1961).

(14) McWhirter, J. R., and W. A. Lloyd, "Controlled Cycling in Distillation and Extraction," Chem.

Eng. Progr., 59, 58 (1963).

(15) Prince, R. G. H., and B. K. C. Chan, "The Seal Point of Perforated Distillation Plates," Trans. Instn. Chem. Engrs. (Australia), 43, T49 (1965).

(16) Robertson, D. C., and A. J. Engel, "Particle Separation by Controlled Cycling," Ind. Eng. Chem., Process Design Develop., 6, 2 (1967).

(17) Robinson, R.G., and A. J. Engel, "An Analysis of Controlled-Cycling Mass-Transfer Operations," Ind. Eng. Chem., 59, 22 (1967).

(18) Schrodt, V. N., J. T. Sommerfeld, O. R. Martin, P. E. Parisot, and H. H. Chien, "Plant-Scale Study of Controlled Cyclic Distillation," Chem. Eng. Sci., 22, 759 (1967).

(19) Sommerfeld, J. T., V. N. Schrodt, P. E. Parisot, and H. H. Chien, "Studies of Controlled Cyclic Distillation: I. Computer Simulations and the Analogy with Conventional Operation," Separation Science, 1, 245 (1966).

(20) Tan, K. S., "A Study of the Dynamics of Cyclic Fixed-Bed Ion Exchange," Ph.D. Thesis, University of Toronto, 1969.

(21) Wade, H. L., C. H. Jones, T. B. Rooney, and L. B. Evans, "Cyclic Distillation Control," Chem. Eng. Progr., 65, 40 (1969).

(22) Zelfel, E., "Zur Stabilitat von Siebboden," Chem. Ing. Tech., 39, 433 (1967).

(23) Zenz, F. A., "How to Calculate Capacities of Perforated Plates," Plates," Petroleum Refiner, 33 (2), 99 (1954).

(24) Zenz, F. A., L. Stone, and M. Crane, "Find Sieve Tray Weepage Rates," Hydrocarbon Processing, 46, 138 (1967).